

1 Sensitivity analysis of input ground motion on surface motion 2 parameters in high seismic regions: A case of Bhutan Himalaya

3 Karma Tempa¹, Komal Raj Aryal², Nimesh Chettri¹, Giovanni Forte³, Dipendra Gautam^{4,*}

4 ¹Civil Engineering Department, College of Science and Technology, Royal University of Bhutan,
5 Phuentsholing, Bhutan

6 ²Faculty of Resilience, Rabdan Academy, Abu Dhabi, United Arab Emirates

7 ³Department of Civil, Environmental and Architectural Engineering (DICEA), University of Naples Federico II,
8 Naples, Italy

9 ⁴Department of Civil Engineering, Institute of Engineering, Thapathali Campus, Kathmandu, Nepal

10 * Correspondance: Dipendra Gautam (dipendra01@tcioe.edu.np)

11 **Abstract.** Historical earthquakes [have](#) demonstrated that [strong motion characteristics and local soil condition](#)
12 [when coupled the combination of the characteristics of strong ground motion and local soil conditions](#)
13 significantly influence [the seismic site response of a particular given site. Most of the Himalayan earthquakes](#)
14 [have depicted anomalous behavior per the site conditions historically. Being one of the most active seismic regions](#)
15 [on earth-, theThe eastern fringe of the Himalaya Mts. is one of the most active seismic areas worldwidehas](#)
16 [observed many devastating earthquakes and uneven damages were extensively reported. To this end, we present](#)
17 [quantification of surface motion parameters for a soft soil deposit located at Phuentsholing city in western Bhutan.](#)
18 [Using one dimensional site response analysis, sensitivity of ground motion variation is estimated for Bhutan. This](#)
19 [study represents the first attempt to quantify the influence of the local site conditions on ground shaking in](#)
20 [Phuentsholing, one of the major commercial hubs of whole Bhutan. To this end, one dimensional \(1D\) ground](#)
21 [response analysis in eight different locations were performed. According to the recent Global Seismic Hazard](#)
22 [Map \(GSHAP\), Phuentsholing Thromde \(city\) in Bhutan is likely to be exposed to the peak ground acceleration](#)
23 [\(PGA\) between 0.20 g – 0.28 g. These high acceleration values do not account for the effect of local site condition](#)
24 [as no instrumental records of past earthquakes are available. This study represents the first attempt to quantify](#)
25 [the influence of the local site conditions on ground shaking in Phuentsholing Thromde \(city\), one of the major](#)
26 [commercial hubs of whole Bhutan. To this end, one dimensional \(1D\) ground response analysis in eight different](#)
27 [locations were performed. TheyThis study accounted for the earthquakes with Magnitude between of moment](#)
28 [magnitude between \$M_w\$ -6.6 and \$M_w\$ -7.5 with a wide variation of PGA-peak ground acceleration \(PGA\) even](#)
29 [beyond 0.28g, which is the maximum PGA range suggested by the Global Seismic Hazard Map \(GSHAP\). In](#)
30 [particular, toTo diagnosedissect the characteristics of six inputted ground motions on eight local ground](#)
31 [conditions, a sensitivity analysis is performed through a statistical analysisstatistically. The statistical correlation](#)
32 [of the response data sets and the linear regression model of the bedrock outcrop and the surface motion spectral](#)
33 [acceleration along the stratified depth waswere examined to quantify the variation in surface motion parameters.](#)
34 [The The studyResults highlighted that those earthquakes ofstrong motions having PGA greater than ~0.34 g](#)
35 [demonstrates greater sensitivity leading to some anomalies in response parameters, resulting in attenuation of](#)
36 [seismic site effect \(amplification\). The same scenario was observed for the PGA range below 0.1g. -with similar](#)
37 [pattern below 0.1 g. The study shows a potential range of seismic site amplification between ~1.7 to 6.2 in Zone](#)

Formatted: Space After: 12 pt

Commented [rev1]: insert the magnitudes

Commented [KT2R1]: Inserted.

38 ~~I and ~1.8 to 5.8 in Zone II over 0.1 s and 3.0 s periods, respectively. This corresponds to the PGA earthquakes~~
39 ~~between 0.11 g and 0.33 g.~~

40 ~~Sensitivity analysis is performed by a statistical correlation function to correlate the ground motion parameters~~
41 ~~for different earthquake shaking intensities. The amplification responses of each soil column are predicted to~~
42 ~~determine the seismic site effects. The study highlights the critical range of the fundamental natural period roughly~~
43 ~~between 0.9 s to ~5.0 s with the highest range of seismic wave amplification between ~2.8 to 6.2, suggesting a~~
44 ~~likely aggravation due to local soil condition that may lead to severe consequences of infrastructure damages.~~

45 **Keywords:** seismic site effect, amplification factor, soil fundamental period, sensitivity analysis, Bhutan.

46 1. Introduction

47 Bhutan ~~falls in Himalaya Mts., is located in the eastern fringe of Hind-Kush-Himalaya, an area vulnerable to~~
48 ~~multiple kind of natural hazards and among them earthquakes are one of the most devastating for the country.~~
49 Historical earthquakes that occurred in ~~this the Hind-Kush-Himalayan~~ region have resulted in enormous losses
50 and damages (Gautam et al., ~~2016~~20167) and thus the impending earthquakes are certain to strike the region with
51 detrimental consequences. The eastern fringe of Himalaya, i.e., Bhutan, and neighboring areas were strongly
52 affected by significant earthquakes in the past, however, most of those occurred ~~in-until~~ the 18th century are not
53 well-documented. The most recent events occurred on April 5th05, 2021 (M_w 5.0) in Samtse (South Bhutan) and
54 on September 2009 Mongar earthquake (M_w 6.7) ~~in eastern Bhutan.~~ ~~The~~ ~~se~~ ~~earthquakes~~ caused major damages
55 in the eastern parts of Bhutan and considerably affected ~~the~~ other parts of the Country (Chettri et al., 2021b).
56 ~~These events and historical records~~ ~~All the past earthquakes~~ highlighted anomalous damage pattern to structures
57 and infrastructures in various parts of the country, especially in the plain areas. ~~Such evidence prompt indication~~
58 ~~of likely local site effects in Bhutan.~~ So far, few studies on local seismic response have been conducted in Bhutan
59 using a single strong motion ~~and they but the studies~~ mainly focused on the role of bedrock depth on ground
60 response parameters (see e.g., Tempa et al., 2020; Tempa, Chettri, Gurung, et al., 2021). ~~In such cases, the~~ ~~The~~
61 ground motion response analysis may not adequately address the accuracy in predicting the response parameters
62 ~~due to limited information regarding site characteristics and their variations within the same soil column~~ (Stevens
63 et al., 2020). ~~In the case of data scarce region such as Bhutan, the variation in terms of material characteristics can~~
64 ~~be possibly accounted for using sensitivity analysis.~~ For this reason, this study ~~is an attempt to quantify~~ ~~quantifies~~
65 the characteristics and effects of ~~different several~~ strong ground motions to ~~seismic responses in the area~~ ~~site effects~~
66 ~~depiction.~~ Seismic ground response analysis fall in the Grade III approach of microzonation studies (e.g. ISSMGE
67 1999; Licata et al., 2018), it is ~~a widely used~~ ~~method widely used~~ by researchers for various applications in order
68 to capture local ground effects or site conditions that can affect the estimate and prediction of ~~the~~ ground motion
69 ~~characteristics~~ (Chavez-Garcia et al., 1990; Lopez-Caballero et al., 2012; Gautam and Chamlagain 2016, ~~and~~ Sil
70 and Haloi 2018). The outcomes of such studies aim to provide local seismic hazard parameters which can be
71 adopted for ~~earthquake resistant~~ design of ~~structures and~~ infrastructures (Douglas, 2006). ~~but also, other~~
72 ~~earthquake hazards such as landslides and soil liquefaction~~ (Bommer and Martinez-Pereira, 2000). ~~These~~
73 ~~ground~~ ~~Ground~~ response parameters typically characterize the complex nature of strong ~~motion~~ accelerograms
74 using a simple expansion of predictive relationships. The two prominent deterministic and probabilistic
75 approaches are widely used for seismic hazard studies globally. ~~Wyss and Rosset, (2013) stated that the standard~~

Commented [rev3]: this is not very clear, try to modify

Commented [KT4R3]: minor edits.

Commented [KT5]: Kindly edit as per reviewer's comments.

Formatted: Numbered + Level: 1 + Numbering Style: 1, 2, 3, ... + Start at: 1 + Alignment: Left + Aligned at: 0" + Indent at: 0.25"

Commented [rev6]: Not clear

Commented [rev7]: ISSMGE (1999) Manual for zonation on seismic geotechnical hazards. In: Technical committee for earthquake geotechnical engineering, TC4, international society for soil mechanics and geotechnical engineering. The Japanese Geotechnical Society, Tokyo

Commented [rev8]: A multi-level study for the seismic microzonation of the Western area of Naples (Italy) Licata, V., Forte, G., d'Onofrio, A., Santo, A., Silvestri, F. Bulletin of Earthquake Engineering, 2019, 17(9), pp. 4711–4741

76 probabilistic seismic hazard assessment method (PSHA) leads to an over or underestimation of the expected
77 acceleration and intensity respectively in areas with low and high seismicity often resulting in incorrect results.
78 Similarly, Previously, Tempa, Chettri, Gurung, et al. (2021) recommended the use of a the deterministic approach
79 that can calculate the accelerations and losses that would occur if the maximum considered earthquake
80 (MCE) estimate parameters under various earthquake occurrence scenarios, occurs. In addition, Notably, selecting
81 a single ground motion by considering only amplitude only for seismic hazard analysis may not be a reliable
82 approach to estimating site amplification. The selection of wide amplitude range and the assessment of likely
83 fluctuation scenario for Bhutan is not done yet. Hence, the ground motion parameters that are related to the
84 amplitude are investigated to examine and predict the variability, often considered regarded as sensitivity,
85 concerning mean values and associated scatter. Although input motion selection is a complex procedure, a simple
86 approach widely adopted is to scale ground motion records to a target spectral acceleration in the fundamental
87 period of the structure of interest (Kramer et al., 2012).

88 ~~To quantify the seismic site effects in terms of amplification of amplitude parameters, a range of time histories~~
89 ~~is selected and site response parameters are estimated.~~ In this paper, sensitivity analysis of site response for
90 specific soil conditions in Phuentsholing, (Bhutan) is explored by a statistical correlation function of the ground
91 motion parameters for different earthquake shaking intensities. The study area is very significant, as Phuentsholing
92 is one of the major urban and commercial hubs in Bhutan Himalaya and seismic site effects on existing structures
93 may have detrimental consequences due to inherent vulnerabilities of structures and infrastructures as well as due
94 to the likely phenomenon such as amplification effects in loose soil deposits presence of loose soil deposits. To
95 quantify the seismic site effects in terms of amplification of amplitude parameters, a range of time histories is
96 selected, and site response parameters are estimated. ~~To quantify the seismic site effects in terms of amplification~~
97 ~~of amplitude parameters, a range of time histories is selected and site response parameters are estimated.~~

98 2. Seismicity and geological setting geology of the study area

99 The Himalayan region is one of the most seismically active zones regions on earth, which observes characterized
100 by both large and moderate-sized events frequently (Drukpa et al., 2006). Bhutan is located in the eastern
101 Himalayas formed due to the subduction of the Indian plate beneath the Eurasian Plate and spans from the low-
102 lying Brahmaputra Plain to the high Tibetan Plateau. Most of the land area of Bhutan is underlain by the Main
103 Himalayan Thrust (MHT), which eovers runs along the entire length of the Himalayan a Arc.

104 Historical earthquake catalogue (see Fig. 1a) indicates that Bhutan has experienced several earthquakes
105 characterized by M_w of moment magnitude greater higher than 5.0 since early 1900, among them, including the
106 1915 Trashingang (M_w 6.6), the 1954 Trashiyangtse (M_w 6.4) in the 2009, Mongar (M_w 6.1) earthquake, which that
107 occurred at 11 km east of Bhutan are the most notable ones. The 2011 Sikkim-Nepal earthquake (M_w 6.9) has
108 also also caused noticeable damage to building stocks in Bhutan (Chettri et al., 2021a). The earthquakes in the
109 vicinity of the study area (Phuentsholing) include the 1981 Dagana (M_w 5.1) earthquake and the 2003 Haa
110 earthquake (M_w 5.5). The most recent event occurred in Samtse in 2021 Samtse (M_w 5.1), which affected
111 Phuentsholing and the neighboring areas with an intensity level of IV in Modified Mercalli Intensity (MMI) scale.

112 Continuity of seismic activities in Bhutan is attributed to The high seismicity of the Bhutan is due to the presence
113 of major shear zones such as the Main Himalaya Thrust (MHT), the Main Boundary Thrust (MBT), the Main

Formatted: Numbered + Level: 1 + Numbering Style: 1, 2, 3, ... + Start at: 1 + Alignment: Left + Aligned at: 0" + Indent at: 0.25"

Commented [rev9]: It is necessary a small inset with location of Bhutan move a) bottom right; inset b) could be removed unless we use it later. Isn t it possible to use the geological map as background?

Commented [KT10R9]: Modified, and superimposed.

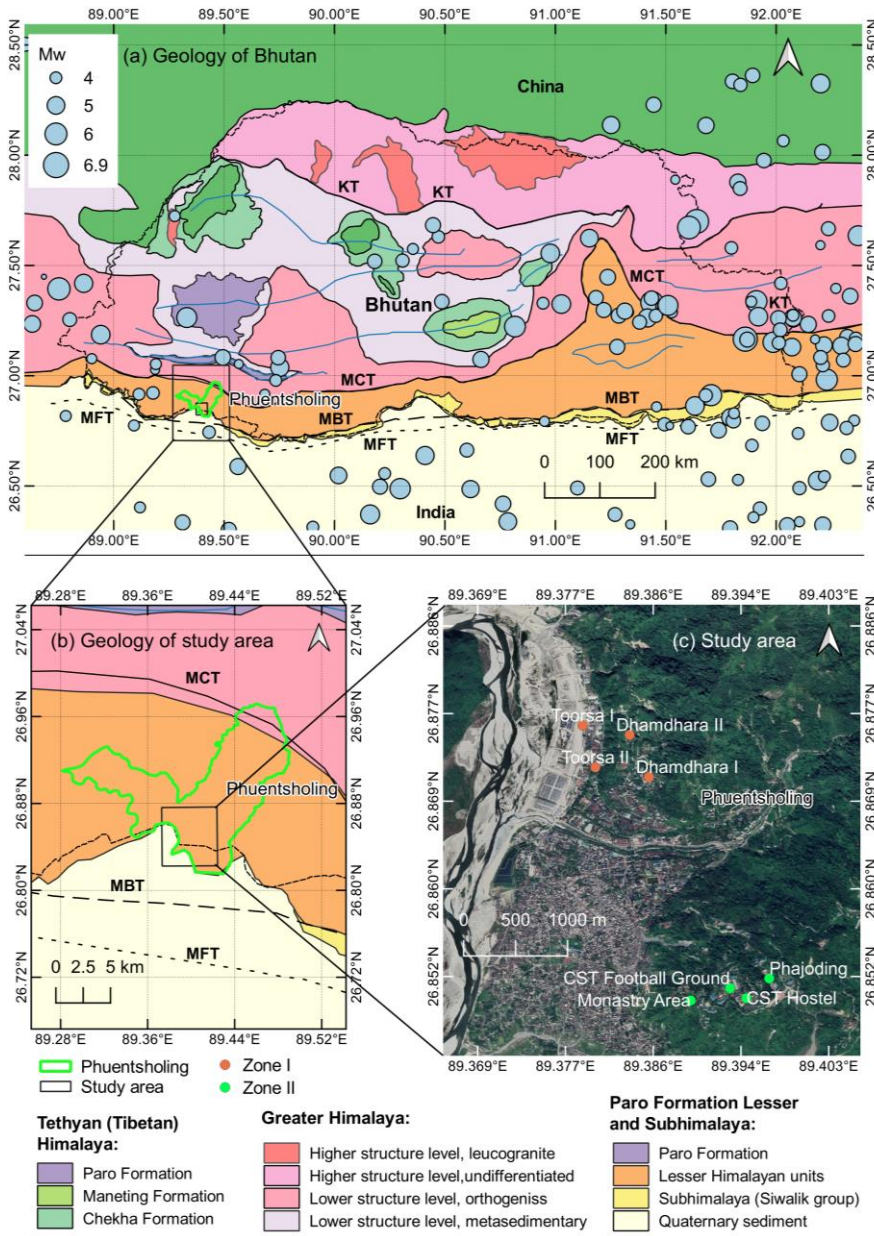
114 Central Thrust (MCT), and the South Tibetan Detachment System (STDS) (Long & McQuarrie, 2010) as shown
115 in Figure 21a. The study area falls underis within the Phuentsholing formation of Buxa group of the Lesser
116 Himalaya mainly made-ofcharacterized by highly weathered dark grey to black slate and phyllite, thin interbeds
117 of limestone; with substantial amount of cream-colored dolomite, and fine-medium quartzite, additionally
118 consisting fine to medium grained conglomeratic quartzite interbedded with phyllite and dolomite towards the
119 Rinchending area of Zone II. Hence, the lithological characteristiecharacteristic of the area indicates weak and
120 highly unstable geology in the region. The pPresence of thrust faults in the proximity of the study area along the
121 entire belt of the Lesser Himalayan units and the quaternary sediments in the south impose-depict the area to be
122 seismically active with the majority of the historical earthquake events occurring-concentrated within these
123 geological units.

124 In particular, this study focuses-focussed on Phuentsholing Thromde (city) under-of Chhukha
125 dzongkhag (district) in Bhutan (Fig. 31c). The city is one of the major commercial hubs for trade with India,
126 making the town the gateway to Bhutan for trade with India. The proposed study area is challenging-because-of
127 theobserving rapid infrastructure development activities and expansion-of-urban-landurban expansion use-to-eater
128 tofor residential, commercial, and industrial transformation-besidespurposes, providing a major trade network to
129 other districts, e.g., extended Toribari township in the east and Amochu Land Development and Township Project
130 (ALDTP) in the west. The Phuentsholing city covers an area of 15.6 km² and is located at 26.86°E and 89.39°N.
131 The city is-populated-with-ahas the population of 27,658 people, mostly distributed towards the peripheral
132 international border area with a total of 2,263 residential and commercial buildings per the 2020 statistics (data
133 are-referred-to-the-year-2020; <http://www.pcc.bt/index.php/>). [The] seismic site characterization includes
134 eight locations in the regions of Dhamdhara, Toorsa, and Rinchending in Phuentsholing, Bhutan. In this study,
135 the sites are grouped into two main zones based on the geographical location and the-proximity-of-the
136 surveyimmediate availability of survey locations. These two grouped-zones also refer to the Local Area Plan
137 (LAP) of Phuentsholing. The zones are Zone I: Dhamdhara I, Dhamdhara II, Toorsa I and Toorsa II, and Zone II:
138 College of Science and Technology (CST) Football Ground, CST Hostel, Phajoding, and Monastery area. ~~Of~~
139 ofAmong the 8 of-these-LAPs, Dhamdhara and Toorsa (Zone I) fall-underare in the same region in the western
140 part of the city and Rinchending (Zone II) in the east. A-similar-classification-was-also-used-by-Tempa-et-al.
141 (Tempa, Chettri, Gurung, et al., 2021). The zones are: Zone I: Dhamdhara I, Dhamdhara II, Toorsa I and Toorsa
142 II, and Zone II: College of Science and Technology (CST) Football Ground, CST Hostel, Phajoding, and
143 Monastery area.

Commented [rev11]: isn t it possible to simplify this map? The name of the formations tell nothing to a foreign reader, it is better a lithological map grouping some formations together; thrusts in red;

Commented [KT12R11]:

Formatted: Space Before: 24 pt, After: 12 pt, Tab stops: 1", Left



144

145 **Figure 1:** [Geology and seismicity](#) and the study area: (a) Geological map of Bhutan reproduced from [McQuarrie](#)
 146 [et al. \(2013\)](#) and seismicity. (b) Location of Phuentsholing and geology of the area. (c) Study area showing
 147 surveyed site using MASW (modified from [Google Earth Pro 2021](#)).

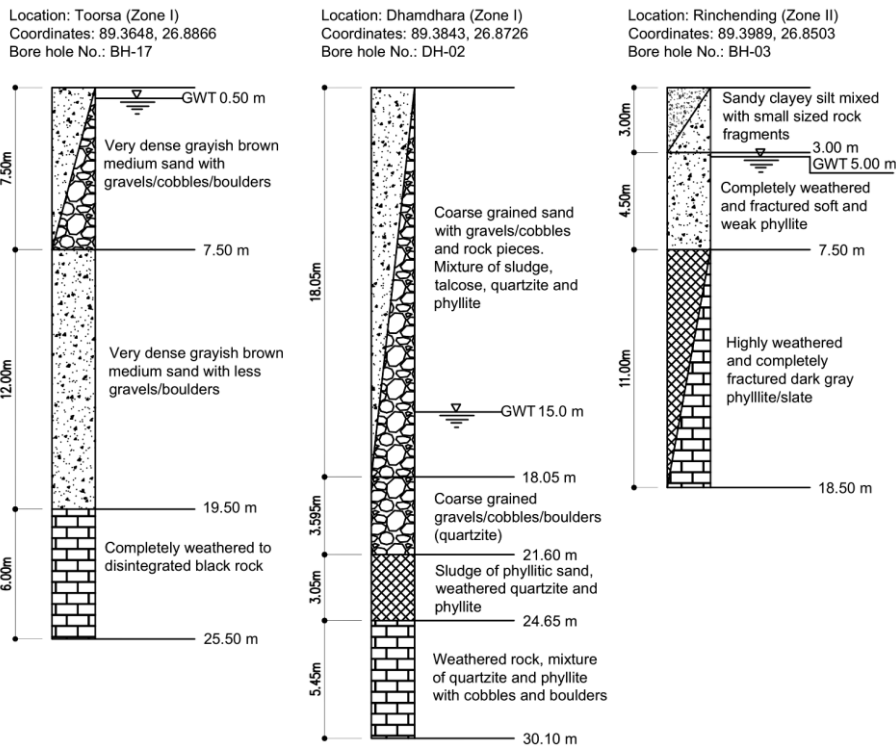
148 **3. Materials and method**

149 **4.13.1 Geotechnical site characterization**

150 The geotechnical reports collected by Phuentsholing municipality provided have 29 stratigraphic logs. From these
 151 records, the depth of the water table (GWT) was derived/demarcated. Drilling log data showed the highest depth
 152 of the water table in the Dhamdhara area at a depth of 12.5 m to 16.0 m, while the whereas groundwater table in
 153 Rinchingding area is at 5 m underlying, followed by the Toorsa area at between 0.5 m and 3m, which is below
 154 located near the riverbed. The depth of the water table is one of the essential input parameters used for 1D ground
 155 response analysis. Three drill holes are presented to typically illustrate the underground stratigraphy (Figure 2).
 156 Table 1 presents a summary of soil properties from laboratory testing of in-situ samples collected from the drill
 157 holes. The number of samples in each zone represents the total number of samples collected from all drill logs at
 158 various stratigraphic depths. All laboratory tests have been verified according to the Indian Standard Codes.
 159 Testing included physical identification, Atterberg limits, grain size distribution curve definition and direct shear
 160 testing. Field tests such as the standard penetration test-resistance (SPT) and core cutter test were
 161 performed to determine resistance to penetration (N-value/SPT-N) and field density, respectively

Formatted: Numbered + Level: 1 + Numbering Style: 1, 2, 3, ... + Start at: 1 + Alignment: Left + Aligned at: 0" + Indent at: 0.25"

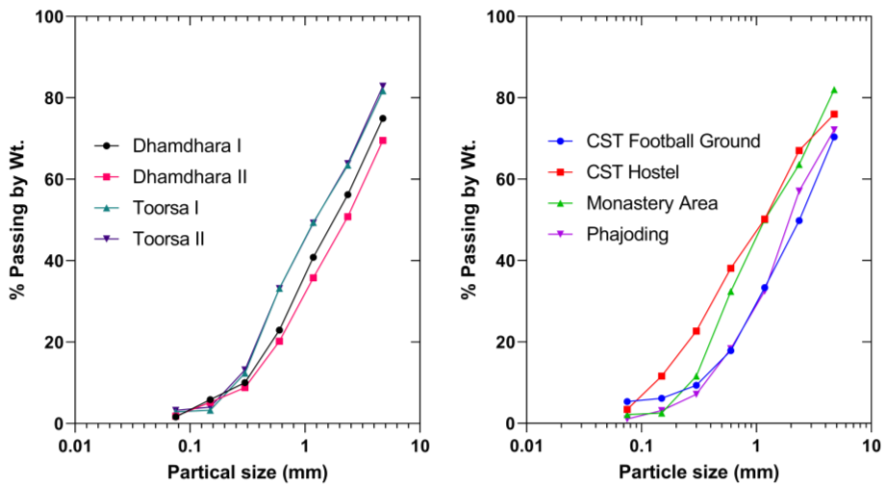
Formatted: Outline numbered + Level: 2 + Numbering Style: 1, 2, 3, ... + Start at: 1 + Alignment: Left + Aligned at: 0" + Indent at: 0.25"



162
163 **Figure 2:** Typical borehole stratigraphy in Toorsa and Dhamdhara (Zone I) and Rinchingding (Zone II).

164 As shown in the stratigraphic logs reported in Fig-5, the shallow soils are the upper strata comprise
 165 predominantly mixed coarse-grained soils characterized by dominant sand with considerable fraction of sand.
 166 consisting of mainly made of sand with a high proportion of gravel and a good proportion of fines. Something
 167 similar was also reported by some studies that were carried out in the study area indicating similar to the finding
 168 of previous studies (Tempa and Chettri, 2021; Tempa, Chettri, Sarkar, et al., 2021). The soil classification of the
 169 Phuentsholing area carried out by sieve analysis highlighted that most soils consist of 22.74% gravel, 74.89%
 170 sand, and 2.37% of the silt and clay fractions. The sieve analysis results for the respective zones are shown in Fig.
 171 63. The soils in Toorsa are non-plastic, as coarser grained soils dominate the particle distribution, while the soils
 172 in Rinchening and Dhamdhara have a low plasticity with a plasticity index (PI) of 6.5 and 10, respectively. The
 173 bulk density is 1.8 g/cm³ in Toorsa, 1.64 g/cm³ in Dhamdhara, and 1.33 g/cm³ in Rinchening. The shear strength
 174 parameter, cohesion (c), ranges between 0-0.18 kg/cm², while the angle of internal friction (ϕ) in the study area is
 175 up to 35°.

Formatted: English (India)



176
 177 **Figure 63:** Results of sieve analysis showing grain size distribution curves. Representative grain size distribution
 178 curve for the study area.

Commented [rev16]: Can we group them in 1 fig? We can color the curves of the same color for each zone.

179 **Table 1.** Average soil parameters in the study area.

Commented [KT17R16]: Consolidated to 1 fig.

Location	Testing methods	Soil parameters	No. of samples	Reference
Toorsa (Zone I)	Atterberg's limit	Non-plastic	86	IS: 2720 (Part 5)-1995
	Core cutter	Bulk density, $\gamma_t = 1.8$ g/cc Dry density, $\gamma_d = 1.64$ g/cc		IS:2720 (Part 29)-1975
	Direct shear	$c = 0$ $\phi = 35^\circ$		IS: 2720 (Part 13)-1997
	SPT	N -value = 25 to 50		IS: 2131-1981
Dhamdhara	Atterberg's limit	Low plasticity (PI = 6.5)	28	IS: 2720 (Part 5)-1995

Commented [rev18]: Can't we insert a 3rd zone?, so Toorsa and Dhamdhara are representative of different areas. For what I see on google they should be quite different.

(Zone I)	Core cutter	Bulk density, $\gamma_t = 1.64$ g/cc Dry density, $\gamma_d = 1.51$ g/cc	26	IS:2720 (Part 29)-1975
	Direct shear	$c = 0.073$ kg/cm ² $\phi = 31.44^\circ$		IS: 2720 (Part 13)-1997
	SPT	N -value = 19 to 37		IS: 2131–1981
Rinchending (Zone II)	Atterberg's limit	Low plasticity (PI = 10)	26	IS: 2720 (Part 5)-1995
	Core cutter	Bulk density, $\gamma_t = 1.83$ g/cc Dry density, $\gamma_d = 1.70$ g/cc		IS:2720 (Part 29)-1975
	Direct shear	$c = 0.18$ kg/cm ² $\phi = 20-30^\circ$		IS: 2720 (Part 13)-1997
	SPT	N -value = 21 to >100		IS: 2131–1981

180 Shear wave velocity profiles from eight locations in the study area based on the multispectral surface
181 wave analysis Multispectral Analysis of Surface Waves (MASW) (Fig. 7) and empirical correlation developed by
182 Tempa et al. (Tempa, Chettri, Gurung, et al., (2021) are used to carry out ground response analysis.
183 According to the shear wave velocity profile, the engineeringengineered bedrock ($V_s > 800$ m/s) lies at a depth
184 ranging from of 150 m to 400 m (e.g., Dhamdhara I in Zone I and Phajoding in Zone II), as shown in Fig. 84.
185 According to the parametric analysis carried out by Tempa et al. (Tempa et al., (2020) in the study area, the site
186 condition in the study area is classified into ground as ground type B in conjunction to per the Euro Code EC-08
187 and National Earthquake Hazards Reduction Program (NEHRP) with the majority of shear velocity ($V_{s,30}$) ranging
188 between 380–470 m/s, except in for the Phajoding, which has a shear wave velocity of 584.76 m/s (Table 2). The
189 $V_{s,30}$ can be estimated with the following using Equation 1.

$$V_{s,30} = 30 \sqrt{\sum_{i=1}^N \left(\frac{h_i}{V_i} \right)^2}, \text{ m/s}$$

(1)

193 **Table 2.** Site classification as per Euro Code EC-08

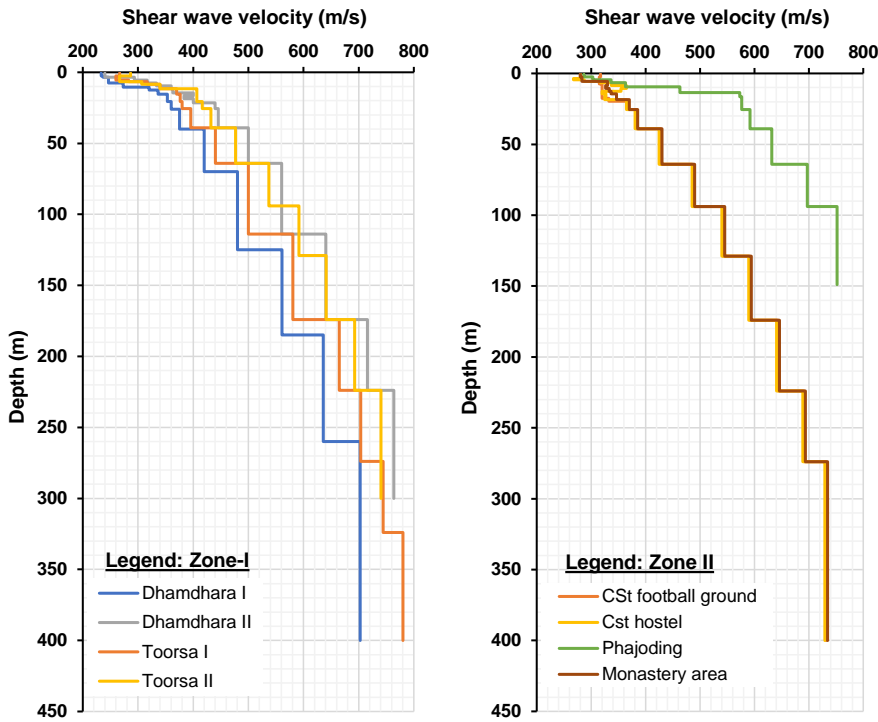
Zones	Sites	$V_{s,30}$ (m/s)	Ground Type
I	Dhamdhara I	386.43	B
	Dhamdhara II	435.92	B
	Toorsa I	439.54	B
	Toorsa II	464.30	B
	CST football ground	426.76	B
II	CST hostel	426.61	B
	Monastery area	446.20	B

Commented [rev19]: are they used on spt ? we should locate them as well

Commented [KT20R19]: No SPT. MASW locations are indicated in Fig 2.

Formatted: Justified, Indent: First line: 0.5", Space Before: 0 pt, After: 0 pt

	Phajoding	584.76	B
All	Bedrock	>800	A



194

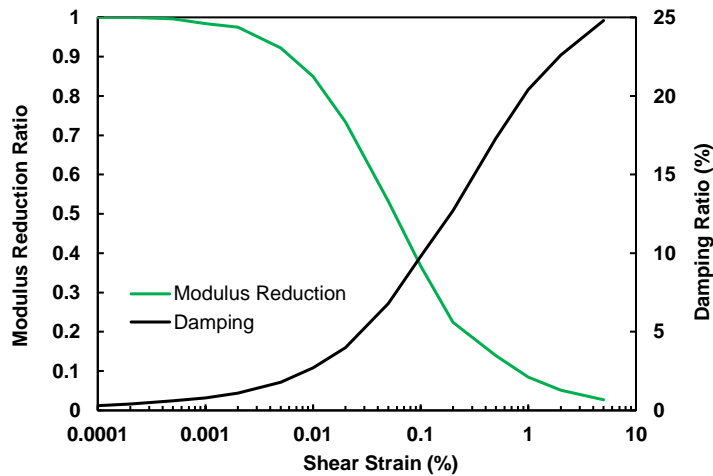
195 **Figure 8.4:** Shear wave velocity profile of study locations in Phuentsholing, Bhutan.

196 ~~To further supplement to complement the requirements for the seismic demand action and~~
 197 ~~damage risk, it is essential to take into account consideration of the subsurface conditions associated with the~~
 198 ~~earthquake energy, which that amplify or abbreviate the ground motion responses is imperative (Kramer, 1996).~~
 199 Dynamic properties of soils are influenced by shear modulus and damping and are defined by the respective
 200 degradation models, regarded as the backbone curves. Figure 9-5 represents the dynamic soil model for sand used
 201 in this study. Degradation models are well established by many ~~researchers-investigators~~ for different types of
 202 soils, ~~which influence affecting~~ the response at low strain levels, (see e.g., (Seed and Idriss, 1970; Vucetic and
 203 Dobry, 1991; Darendeli, 2001; Dobry and Vucetic, 1982; Seed et al., 1986).

204 A damped linear elastic model of the soil system is used for the analysis. Due to ~~the non-linearity of the~~
 205 soil nonlinearity for which the shear modulus is strain-dependent, ProShake performs an iterative process on the
 206 linear model until both the moduli and damping ratios are compatible with the average strains and convergence is
 207 achieved ~~on at~~ the last iteration (Shafiee et al., 2011; Puri et al., 2018). The nonlinear and hysteretic stress-strain
 208 behavior of soils under cyclic loadings is approximated as a function of G_{sec} and G_{max} . This predetermined

Formatted: Indent: First line: 0.5"

209 estimation of G_{sec} or G and G_{max} is attributed by unit weight or bulk density, ρ , and shear wave velocity, V_s (
 210 $G_{max} = \rho V_s^2$). Similarly, damping ratios are predicted as a function of G_{sec} or G values. This estimation is achieved
 211 using the iterative procedure in the Proshake 2.0 program (EduPro Civil Systems Inc., 2017).



212
 213 **Figure 95:** Average modulus reduction ratio and damping ratio adopted for sand (Seed & Idriss, 1970).

214 **4.23.2 Selection of input motion**

215 ~~The definition of~~ **Defining Definition of** the input motion that ~~should be adopted assumed is considered~~ for site
 216 response analyses of an area requires both ~~the subsoil subsurface~~ characterization and a careful selection of
 217 ~~accelerograms acceleration time histories~~. In Bhutan, records of acceleration time histories are very ~~scarce rare, if~~
 218 ~~not absent, and in~~ the absence of a national seismic code, Bhutan is assumed to fall under Indian seismic zone
 219 IV and V, with an ~~expected maximum~~ PGA of 0.24 g and 0.36 g ~~for design purposes, respectively, for Maximum~~
 220 ~~Considered Earthquake (MCE) (IS:1893, 2002), and In in many cases, PGA of 0.36 g is applied uniformly across~~
 221 ~~the whole country (Stevens et al., 2020)~~. For the two zones mentioned, the PGA for earthquakes with a return
 222 period of 475 years is expected to be half of ~~the MCE maximum considered earthquake (MCE)~~, i.e., 0.12 g and
 223 0.18 g. ~~Notably, the GSHAP depicts the PGA range between 0.2-0.28g. From the global seismic map (GSHAP),~~
 224 ~~the PGA depicted are in the presented range from 0.20 g to 0.28g, with an increasing pattern trend to in~~ the east of
 225 the country (Tempa, Chettri, Gurung, et al., 2021). The discrepancies in such agreements without much
 226 conformity lead to a question about how ~~differently~~ the earthquake scenario is ~~differently~~ distributed at the
 227 regional level at the current ~~this~~ juncture. In this study, such observations have been ~~were~~ instrumental in the
 228 ~~Considering the variations in expected PGA, we selected~~ of six ~~acceleration time histories historical global~~
 229 ~~earthquakes as input motions having an intensity of with a PGA intensity in the range of ranging from~~ 0.067 g to
 230 0.422 g, considering the ~~least lowest~~ and the highest range of possible earthquake scenarios (Table 3).
 231 ~~Two properties of seismic motion are most common for engineering purposes. Most commonly, for engineering~~
 232 ~~purposes, two characteristics of earthquake motion, i.e., amplitude and frequency content of the motion at bedrock~~
 233 ~~level motion are, of primary importance (Kirtas et al., 2015; Kramer, 1996)~~. The acceleration time histories used

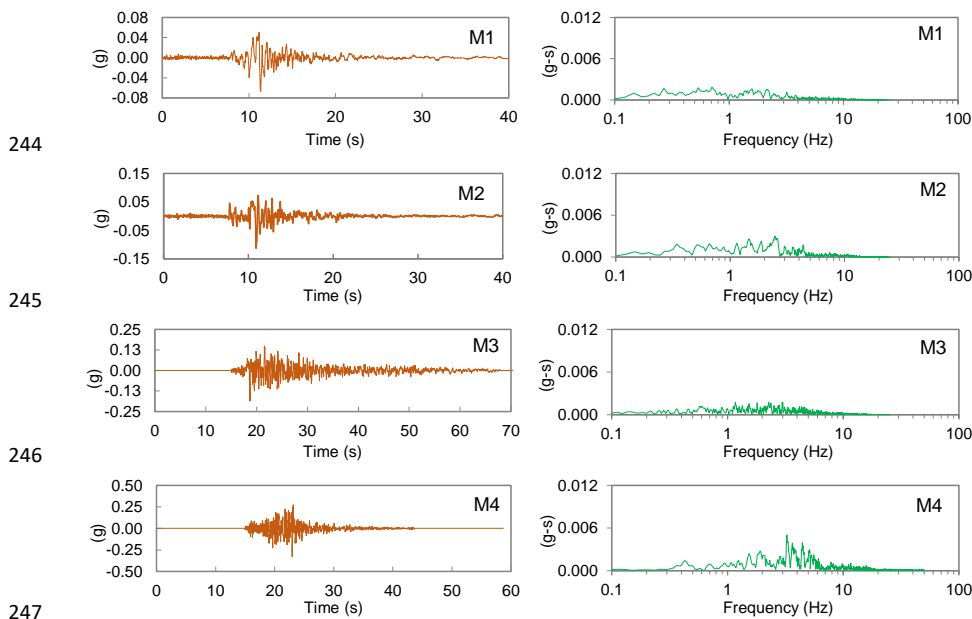
Formatted: Outline numbered + Level: 2 + Numbering
 Style: 1, 2, 3, ... + Start at: 1 + Alignment: Left +
 Aligned at: 0" + Indent at: 0.25"

Formatted: Indent: First line: 0", Space After: 0 pt

234 for the 1D ground response analysis are shown in Fig. 40-6 in ascending order of PGA order using the ProShake
 235 2.0 computer program. In the ProShake 2.0 program, input motion and soil profile are denoted as “M” and “P”
 236 respectively, and are used-annotated in the following-subsequent sections (Table 3). The amplitude and frequency
 237 content of the bedrock level motion are particularly the most important parameters (Kirtas et al., 2015; Kramer,
 238 1996). To understand the strong ground motion characteristics, we have-plotted the Fourier amplitude versus
 239 period in the frequency domain (or period), which represents representing the Fourier amplitude spectra of the
 240 input motions, as shown in Fig. 406. The effect of local soils is indicative at a much higher frequency range in all
 241 the investigated sites.

242 **Table 3. Historical earthquakes considered as input motion** Selected strong motion records for ground response
 243 analysis.

Event	Station	Year	M _w	PGA (g)	Notation
Loma Prieta/Santa Cruz Mountains	Yerba Buena Island, CA – US Coast Guard	1989	6.9	0.067	M1
Loma Prieta	Diamond Heights	1989	6.9	0.113	M2
Taft Kern County	Taft	1952	7.5	0.185	M3
Northridge	Topanga Fire Station	1994	6.7	0.329	M4
El Centro	Imperial Valley Irrigation District	1940	6.9	0.344	M5
Petrolia	Cape Mendocino	1992	6.6	0.422	M6



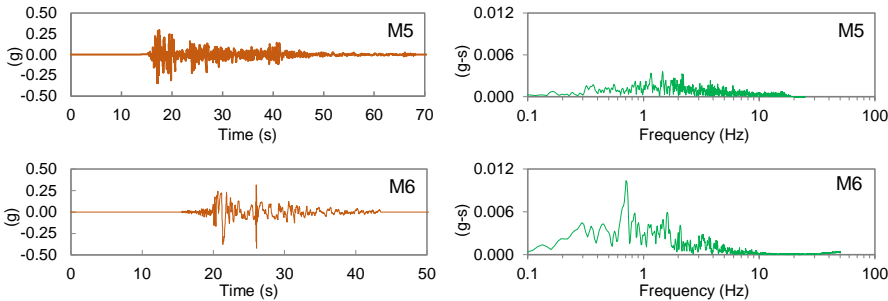


Figure 106: Plot of time histories and corresponding Strong motions and corresponding Fourier amplitude plots of the input ground motions.

4.3.3.3 1D ground response analysis

A 1D equivalent linear analysis was performed at eight sites in Phuentsholing, Bhutan to estimate local site effects with using the ProShake 2.0 program. In this study, six strong motion records were used to replicate low, medium, and high earthquake seismic acceleration categories based on the intensity of PGA. The ProShake 2.0 program offers provides the flexibility to input ground motions and soil profiles and is handy useful to for estimate estimating the outcrop responses to input ground shaking. The improved shear wave velocity profiles down to the engineered bedrock depth (150 m and 400 m) from eight sites were used, which is reported in the study by Tempa et al. The enhanced shear wave velocity profiles to the depth of the engineering bedrock (150 m and 400 m) of eight locations based on initial MASW profiles of ~22.2 m depth is well established in the study conducted by Tempa et al. (Tempa, Chettri, Gurung, et al., 2021). These deep shear wave profiles used in this study incorporate are a complementary supplemental input parameter in the current study, which considers the effects of depth and soil type of varying visco-elastic soil strata layers underlain with by above the predicted engineering bedrock. The 1D ground response analysis takes into accounts for wave propagation from the bedrock outcrop through the visco-elastically layered-stratified soil deposit and provides an estimate of the ground-surface motion parameters at surface. The complex response method is solved by the equation of motion in the frequency domain. The soil-soil nonlinear response soil is estimated by an iterative, quasi-linear procedure in which successive linear analyses are performed, with the soil while updating the shear modulus and damping ratio are updated based on the shear strain level obtained in from the previous preceding iteration. analysis. Iterations continue until the strain-compatible modulus and damping converge.

1.4. Results and discussion

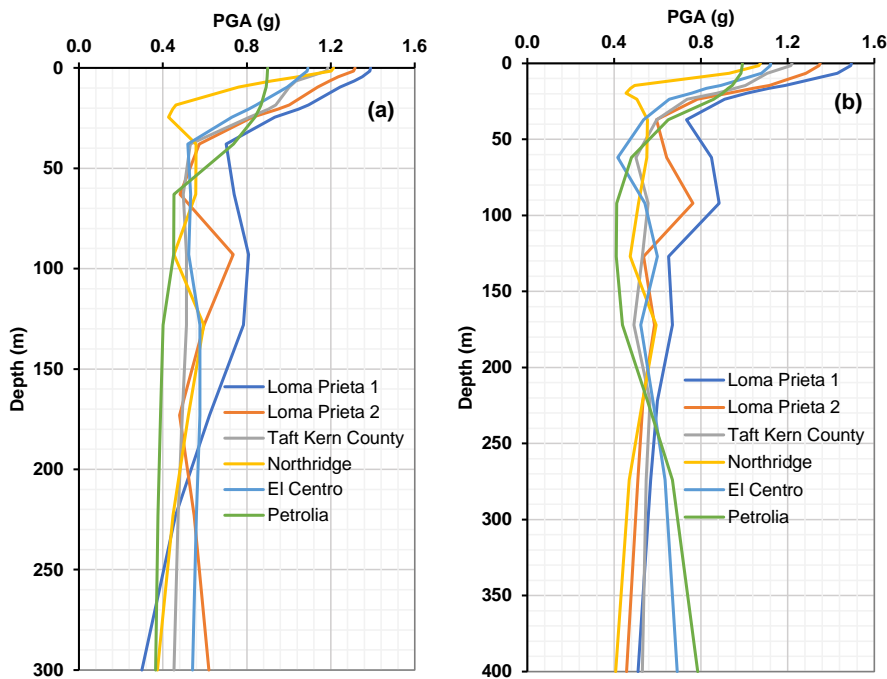
4.4.1 Seismic site effects

Figure 7 shows normalized surface PGAs PGAs on surface at two typical locations of two the investigated zones. The chart shows approximately depicts PGA of 1.2 g to 1.5 g for low intensity PGA earthquakes, 0.7 g to ~1.1 g for medium and high intensity PGA earthquakes. Response parameters can be defined and characterized based on the amplitude parameters of the ground motion and the severity of the ground motion excitation in nearby structures. to on the respective structure. This in turn

Formatted: Outline numbered + Level: 2 + Numbering Style: 1, 2, 3, ... + Start at: 1 + Alignment: Left + Aligned at: 0" + Indent at: 0.25"

Formatted: Indent: First line: 0"

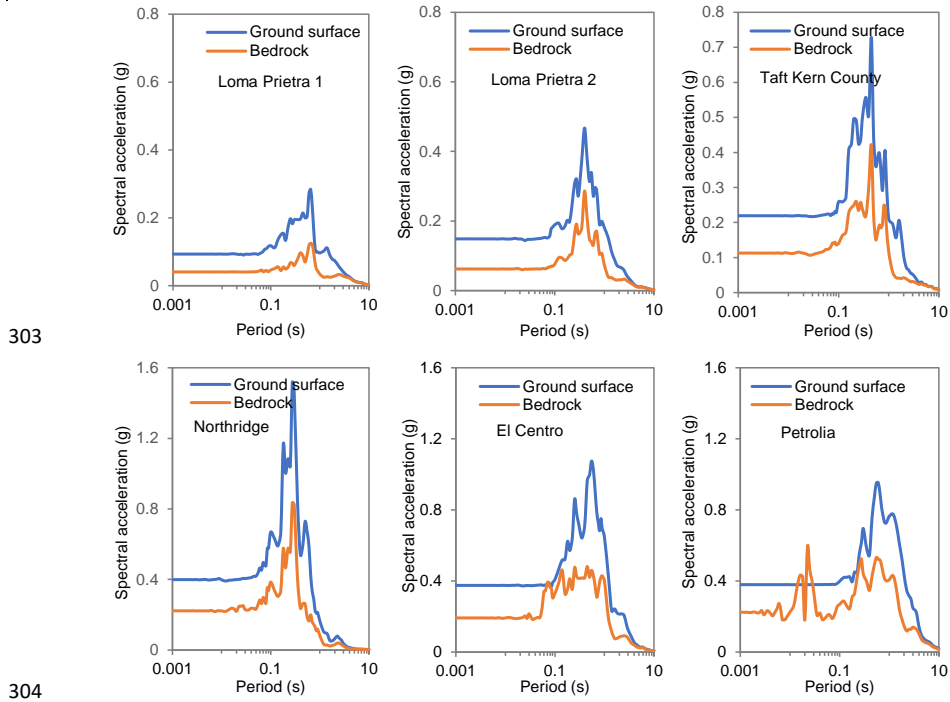
278 is a function of the amplitude or intensity, the frequency content, and the duration of the ground motion (Bradley,
 279 2011). Natural periods or frequency domain parameters are well related to the seismic behavior of structures and
 280 indirectly reflect the ground motion characteristics (Zafarani et al., 2020). Hence, to commensurate this
 281 relationship, the response spectrum plot of bedrock and surface motion is are presented in Fig. 8 and 9. The results
 282 to of various input ground motions indicate a higher spectral acceleration of the soil profile in the period range
 283 from between 0.3 s to 3.0 s with the peak spectral acceleration of approximately 0.14 g to 1.62 g. Thus, the
 284 structures with similar fundamental vibration period are likely to be exposed to greater peak spectral acceleration.
 285 peak spectral acceleration. Buildings 3 m to 30 m tall usually fall into this spectrum. In the city of Phuentsholing,
 286 buildings with 2-8 storeys can show higher values of hazard responses due to the variability of the earthquake
 287 shaking intensity and soil condition examined. Both study areas show a similar tendency of ground responses.
 288



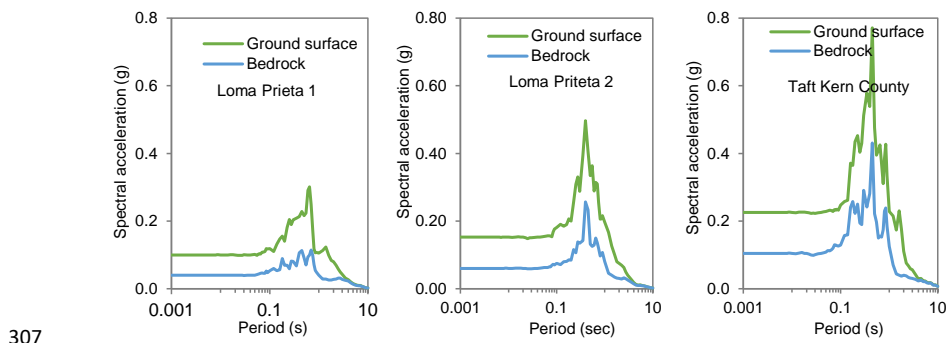
289
 290 **Figure 7:** The typical profiles of normalized peak ground acceleration (PGA), (a) Toorsa II in Zone I, and (b)
 291 CST Football Ground in Zone II.

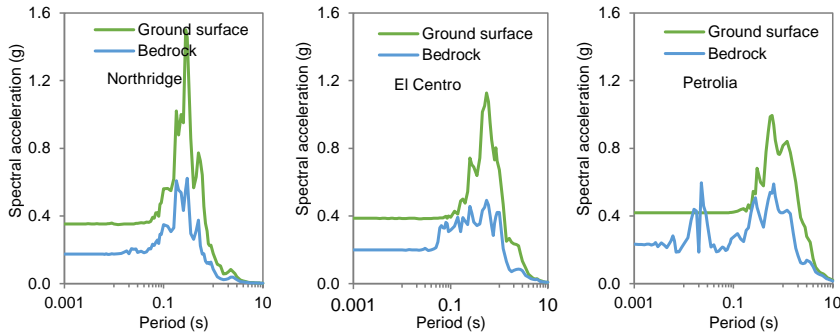
292 Response parameters can be defined and characterized based on the amplitude parameters of the ground
 293 motion and the severity of the ground motion to on the respective structure. This in turn is a function of the
 294 amplitude or intensity, the frequency content, and the duration of the ground motion (Bradley, 2011). Natural
 295 periods or frequency domain parameters are well related to the seismic behavior of structures and indirectly reflect
 296 the ground motion characteristics (Zafarani et al., 2020). Hence, to commensurate this relationship, the response
 297 spectrum plot of bedrock and surface motion is presented in Fig. 8 and 9. The results to various input ground

298 motions indicate a higher spectral acceleration of the soil profile in the period range from 0.3 s to 3.0 s with
 299 approximately 0.14 g to 1.62 g peak spectral acceleration. Buildings 3 m to 30 m tall usually fall into this spectrum.
 300 In the city of Phuentholing, buildings with 2-8 storeys can show higher values of hazard responses due to the
 301 variability of the earthquake shaking intensity and soil condition examined. Both study areas show a similar
 302 tendency of ground responses.



305 **Figure 8:** Typical spectral acceleration of bedrock and ground surface motion at Toorsa II in Zone I corresponding
 306 to the respective input motions.





308
 309 **Figure 9:** Typical spectral acceleration of bedrock and ground surface motion at CST Football Ground in Zone II
 310 corresponding to the respective input motions.

311 ~~A key parameter to account for seismic wave modification by local site conditions is commonly~~
 312 ~~represented by the amplification factor (Bhutani and Naval, 2020). Figures 10 and 11 show the results of typical~~
 313 ~~amplification factors at two locations in the study area. The ratio of the spectral acceleration of the surface motion~~
 314 ~~to the spectral acceleration of the bedrock provides the amplification factor, which according to Eq. 2:~~

$$Amp(T) = \frac{SA_{Soil}(T)}{SA_{Rock}(T)}$$

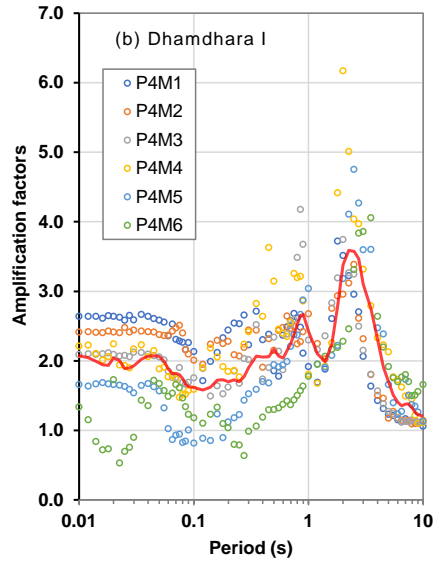
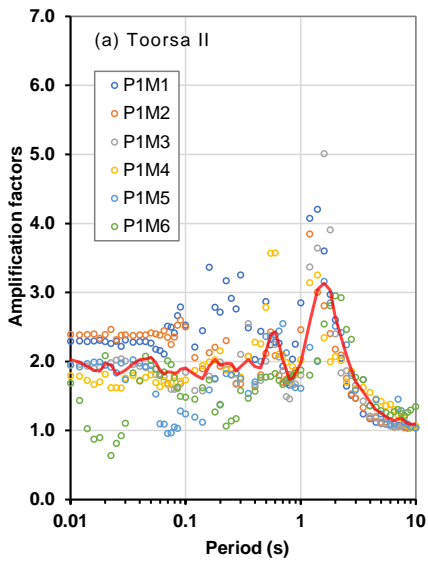
316 (2)

317 ~~From the results of the ground response analysis, the amplification factors in the study areas can be~~
 318 ~~roughly classified into three categories as low, medium, and high ranges, and the average values are highlighted.~~

319 The amplification factors range from 0.7 to 2.7, 0.6 to 2.6, 0.75 to 2.5, and 0.7 to 3.2 for Toorsa II, Dhamdhara I,
 320 CST football ground, and Phajoding respectively for 0.01 s to 0.1 s natural period. In the natural period range
 321 from 0.1 to 1.0 s, the amplification factors are in the range from 1.1 to 3.6, 0.7 to 4.2, 1.0 to 3.7, and 1.2 to 5.2 for
 322 Toorsa II, Dhamdhara I, CST football ground, and Phajoding, respectively. In the high natural period range, the
 323 amplification factors are 5.0, 6.2, and 5.8 for Toorsa II, Dhamdhara I, and CST football ground, respectively.
 324 However, in the Phajoding the ~~significance of the amplification~~ amplification factor is ~ 1.7 due to a much stiffer
 325 soil deposit ($V_{s,30} = 584.76$ m/s) and shallow engineering bedrock at 150 m.

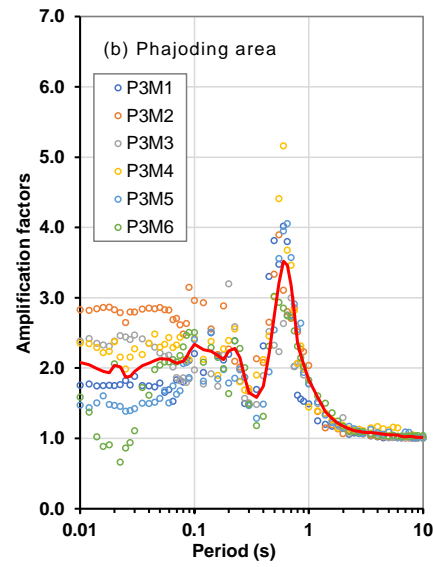
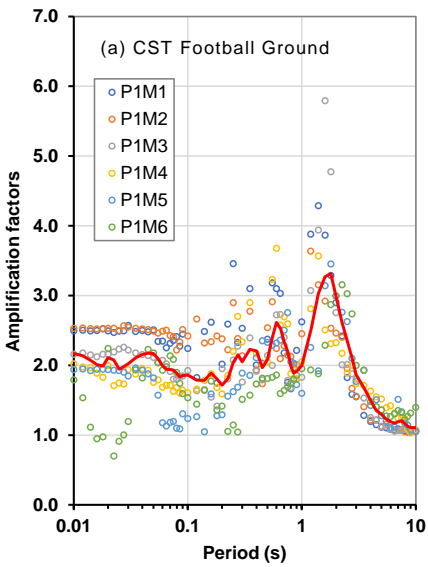
Formatted: Indent: First line: 0.5", Space After: 8 pt

Formatted: Space After: 8 pt



326

327 **Figure 10:** Typical Examples of amplification factors for various earthquakes at (a) Soil profile P1 at Toorsa II
 328 in Zone I, (b) Soil profile P4 at Dhamdhara I in Zone I



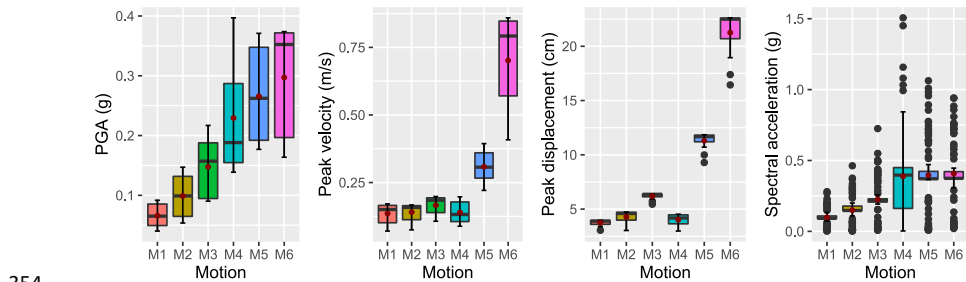
329

330 **Figure 11:** Examples of typical amplification factors for various earthquakes at (a) Soil profile P1 at CST Football
 331 Ground in Zone II, (b) Soil profile P3 at Phajoding in Zone II

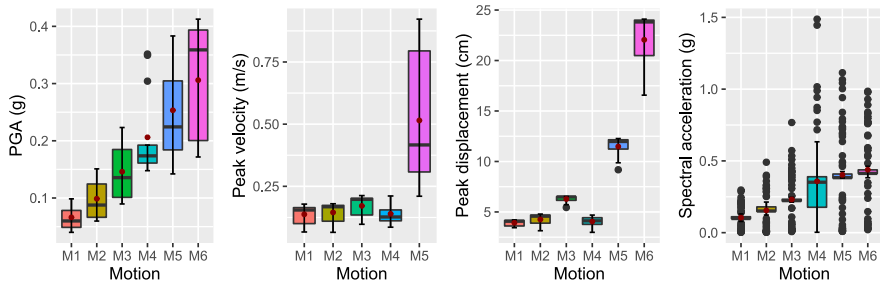
332 **4.5.4.2 Correlation analysis**

333 The main objective of this study is to demonstrate the sensitivity of six earthquakes of different PGA
 334 magnitudes input motion amplitudes to predict the variability of seismic site effects due to local ground conditions.
 335 To achieve this, we first performed a statistical analysis using the results of the 1D ground response analysis. The
 336 fundamentals of statistical analysis are to We aim to examine potential trends, patterns, and relationships between
 337 data sets for the results obtained from the analysis. A statistical quantitative approach is implemented and the
 338 statistical data distribution of the amplitude parameters Using statistical analysis, variation of amplitude
 339 parameters of the input ground motions is are is projected by a box plots (Figs. ure 12 and 13). Hence, Sstatistical
 340 correlations are fitted between pPeak gGround aAcceleration (PGA), pPeak gGround vVelocity (PGV), pPeak
 341 gGround dDisplacement (PGD), and sSpectral aAcceleration (S_a) to determine the interplay correlation between
 342 the effects of strong ground motion and the local soil conditions. As anticipated, the 1992 Petrolia earthquake
 343 with 0.422 g PGA ($M_w = 6.6$) led to the highest-greatest response. However, the 1994 Northridge earthquake
 344 with a PGA of 0.329 g ($M_w = 6.7$) shows greater variability in spectral acceleration compared to other
 345 earthquakes. This is the most relevant finding and perhaps also the most significant in the current study. This is
 346 because the spectral acceleration is one of the most important response parameters corresponding to the interaction
 347 between the ground and the shaking intensity of an earthquake and is directly related to the response of equivalent
 348 SDOF systems. Therefore, from the perspectives of seismic site effects the box plot of the spectral acceleration
 349 (period or frequency domain) is highly scattered with the outliers, confirming uncertainty in the ground response
 350 characteristics in both zones both regions. These indicates that the seismic site effects are likely to increase due
 351 to ground response local soil conditions and could severely affect buildings coinciding with the natural
 352 fundamental frequency. The El Centro and Petrolia earthquakes, with the highest PGAs in this study, also appear
 353 to be closely associated with spectral acceleration.

Commented [KT21]: Revised version and updates with additional linear regression model of bedrock amplitude parameter and surface motion.

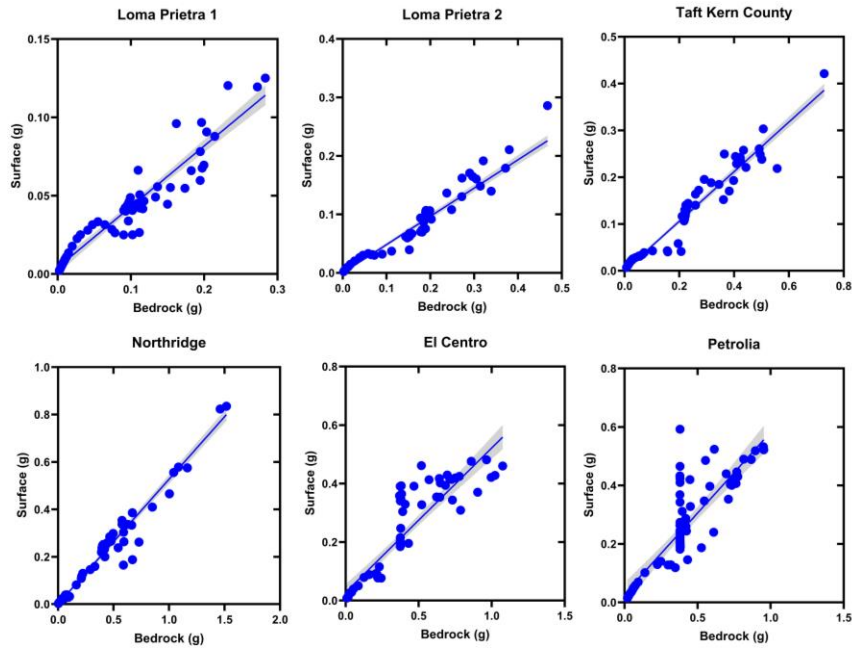


354 **Figure 4912:** Box and Whisker plot for ground motion parameters of soil profile at P1 Toorsa II in Zone I.
 355



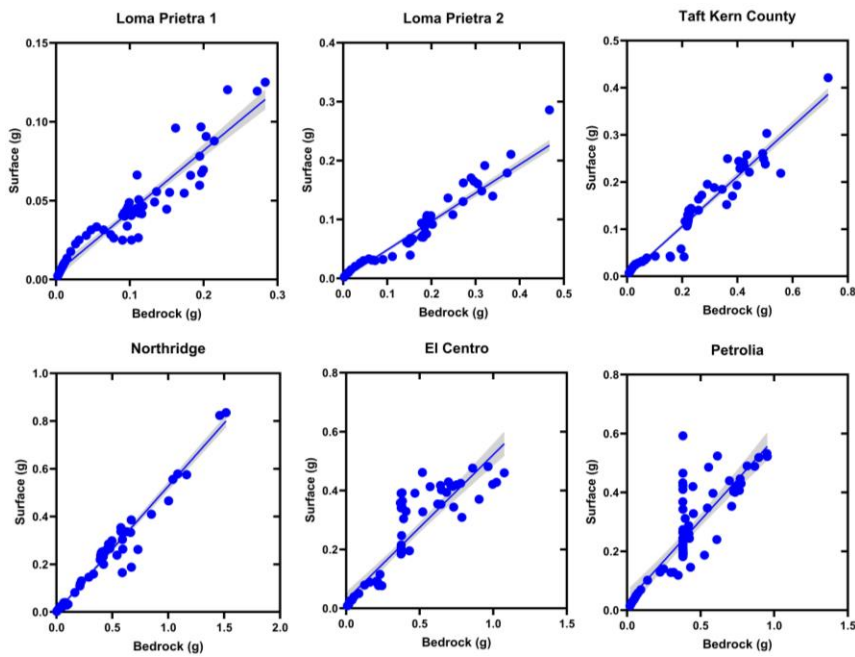
356
 357 **Figure 2013:** Box and Whisker plot for ground motion parameters of the soil profile at P1 CST Football Ground
 358 in Zone II.

359 Primarily, propagating energy waves (outcrop motion) act on each stratified soil layers which that amplifies or de-
 360 amplifies the ground motion response parameters at each stratified soil-layer. The sensitivity of the input motions
 361 is critically monitored, and enhanced correlation are exploited developed. To bring this issue to
 362 surface outline this, a linear regression model for bedrock outcrop motion and the predicted motion parameters as
 363 a function of bedding depth was developed in addition to the statistical parameters presented above. Regression
 364 analysis is performed for one particular soil profile from two zones (Toorsa II and CST Hostel) in order to
 365 accurately substantiate the sensitivity analysis (Figs. 14 and 15).



366
 367 **Figure 14:** Bedrock-linear regression model for bedrock and surface spectral accelerations for Toorsa II
 368 (Zone I)

369 The 95% confidence interval (CI) shows a linear relationship for the historic-Loma Prieta 2-2, Taft Kern County,
 370 and Northridge earthquakes, indicating a closer impact on surface motion that corresponds to outcrop motion.
 371 For In this case, the predominant frequency content of the input motion is between 1 and 10 Hz. (see Fourier
 372 amplitude). In contrast, the Loma Prieta 1, El Centro, and Petrolia earthquakes, with a predominant frequency
 373 between 0.3 and 1.2 Hz, exhibit typical nonlinearity throughout the spectral range, indicating possible damping
 374 of the spectral responses of the soil deposits.

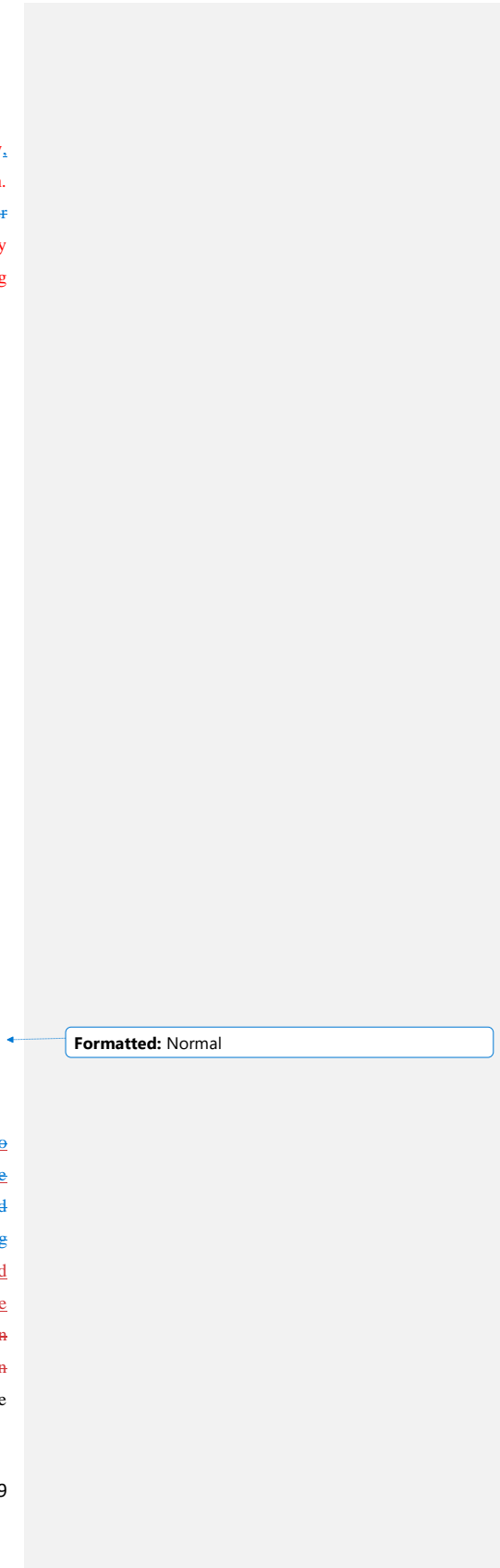


375
 376 **Figure 4615:** Bedrock linear regression model for bedrock and surface spectral accelerations for CST
 377 Hostel (Zone II)

378 4.6

379 **4.74.3 Sensitivity of input motion**

380 The number of response parameter variations on due to different input motion provides addition insight into
 381 sensitivity. As the different seismic ground motions propagate through different soil layers, the ground surface
 382 motion response is modified in an increasing order of magnitude of PGA. As the various earthquake ground
 383 motion propagate through different soil profiles, the ground surface motion response is modified in the ascending
 384 order of the PGA of input motion. Since all analysis sites fall under there in tType B site, the trend of ground
 385 motion variation to surface is very similar, so the average values may be crucial for better implementation of the
 386 scenario-based seismic risk in the study area. Since all the sites fall under the type B site, the trend of the variation
 387 in the ground motion to surface is very similar, so the average values may be decisive for improving the realization
 388 of the scenario-based seismic risk in the study area. Ground response parameters such as PGA and response



Formatted: Normal

389 spectrum intensity including Arias intensity show linear variations for aggregated values with while increasing
 390 intensity of earthquake shaking corresponding to a particular given soil profile. However, the predominant period
 391 opposite linear correlation with the characteristics of strong ground motion. These results were mainly observed
 392 due to change in characteristics of seismic waves propagating through different stratified soil deposits before the
 393 strong ground motion reach the ground surface. In ProShake 2.0, the The mean, median and standard deviation of
 394 the output parameters are computed using regression statistical analysis, and The response spectrum intensity is
 395 computed based on Housner approach (Housner, 1959) as integral from 0.1 to 2.5 s of the pseudo-velocity
 396 spectrum that provides an indication of the average velocity for most civil engineering structures. The plot of
 397 sensitivity of various input motions on amplitude parameters to different local soils in two study zones is shown
 398 in Figs. 16 and 17.

399 The standard deviation is lower for a set of predominant natural periods for a soil profile compared to
 400 the response spectrum dataset and this deviation from the mean value Within the set of predominant natural
 401 periods corresponding to each input motion, the standard deviation is lower compared to the data set of the
 402 response spectrum of the soil column, which indicates a higher strength of stronger soil response to the SDOF
 403 systems, as presented shown in Figs. 16 and 17 Table 4 and Table 5. The non-linearity of soils Soil nonlinearity
 404 often shows a significant scatter in spectral acceleration at higher and lower periods, and therefore the practical
 405 reliability of the result is that it requires prompts more analysis with larger sets of many input motions to predict
 406 the mean (or median) response with some level of confidence (Kramer et al., 2012). Tables 4 and 5 summarize
 407 the statistical results of seismic response parameters indicating the sensitivity of various earthquake inputs at local
 408 sites in Zone I and Zone II. The additional ground response parameters are provided in Tables A1 and A2. The
 409 sensitivity of the output results of input motion is shown in Figs. 14 and 15 with examples from two site
 410 locations from two investigated locations. The results of the correlation analysis and the sensitivity plots indicate
 411 that the G input motion ground motion M4 (Northridge) has a significant influence on most of the response
 412 parameters and except M5 (El Centro) show a slight spread of ground response compared to other ground
 413 motions on Arias intensity. The additional ground response parameters are provided in the appendix (Tables A1
 414 and A2).

415 **Table 4.** Descriptive statistics of averaged ground response parameters in Zone I for all four soil profiles
 416 and six input ground motions.

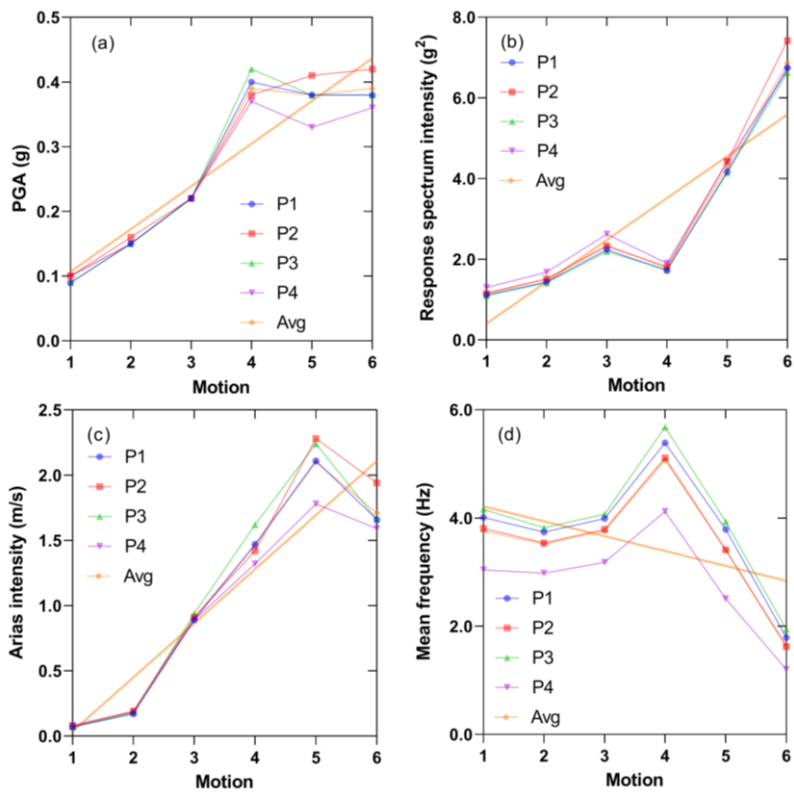
	PGA (g)	Arias intensity (m/sec)	Response spectrum intensity (g ²)	Predominant period (sec)	Mean frequency (Hz)
Mean	0.270	1.073	2.996	0.818	3.527
Median	0.238	0.630	2.450	0.689	3.319
Standard deviation	0.121	0.765	2.013	0.468	1.097
84 th percentile	0.407	2.215	4.541	1.251	4.824
16 th percentile	0.139	0.179	1.322	0.379	2.283

417

- Formatted: Font color: Red
- Formatted: Font color: Red
- Formatted: Font color: Red
- Formatted: Font color: Red

418 **Table 5.** Descriptive Statistical relationship statistics of for averaged ground motion parameters in Zone II for all
 419 four soil profiles and six input ground motions.
 420

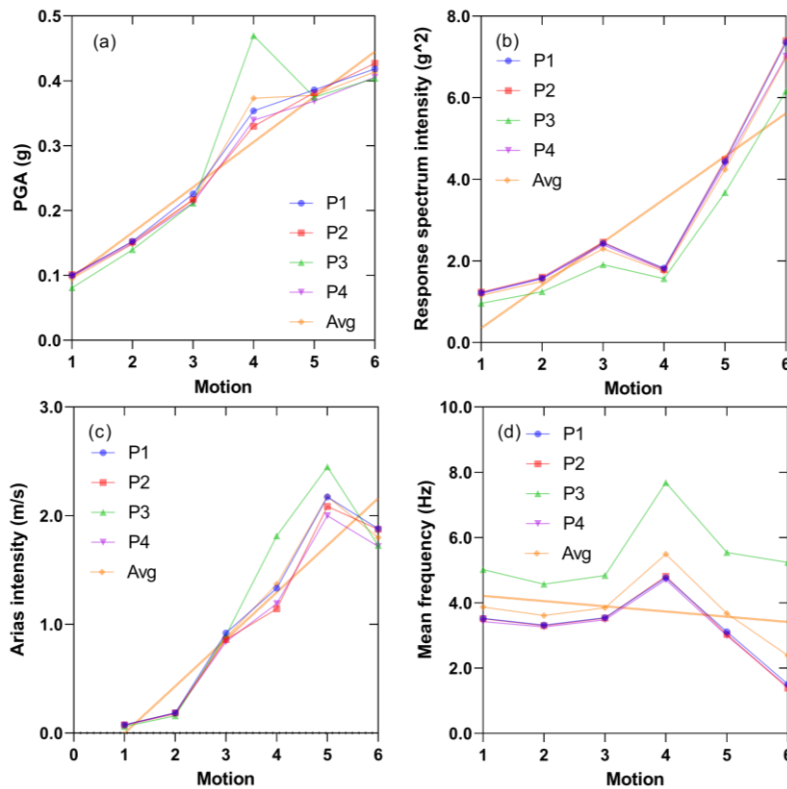
	PGA (g)	Arias intensity (m/s)	Response spectrum intensity (g ²)	Predominant period (s)	Mean frequency (Hz)
Mean	0.271	1.079	2.985	0.812	3.814
Median	0.237	0.622	2.417	0.684	3.538
Standard deviation	0.126	0.794	2.066	0.453	1.382
84 th percentile	0.411	2.226	4.541	1.243	5.330
16 th percentile	0.136	0.174	1.287	0.377	2.349



421

422 **Figure 16:** Sensitivity of input ground motion in Zone I. (a) Peak ground acceleration, (b) Response spectrum
 423 intensity, (c) Arias intensity, (d) Mean frequency. Soil profiles: P1 = Toorsa II, P2 = Toorsa I, P3 = Dhamdhara
 424 II and P4 = Dhamdhara I.

425



426

427 **Figure 17:** Sensitivity of input ground motion in Zone II. (a) Peak ground acceleration, (b) Response spectrum
 428 intensity, (c) Arias intensity, (d) Mean frequency. Soil profiles: P1 = CST Football Ground, P2 = CST Hostel, P3
 429 = Phajoding, and P4 = Monastery area.

430 [Now we speculate that the input motion characteristics of the Northridge earthquake are largely related](#)
 431 [to the potential seismic site effects. The study proposes the implementation of the input motion PGA in the range](#)
 432 [of 0.11 g and 0.33 g of frequency content between 1 to 10 Hz. For the current study. In this study, the PGA of M4](#)
 433 [Northridge are mapped to show the spatial variability in two survey zones as shown in Fig. 18. The PGA in Zone](#)
 434 [I are distributed between 0.37 g to 0.42 g. The variability of PGA in Zone II is higher compared to Zone I, resulting](#)

in the range 0.33 g to 0.47 g. The resulting interplay of strong ground motion with local soil conditions primarily highlights the importance of the current study on the significance of input motion characterization.

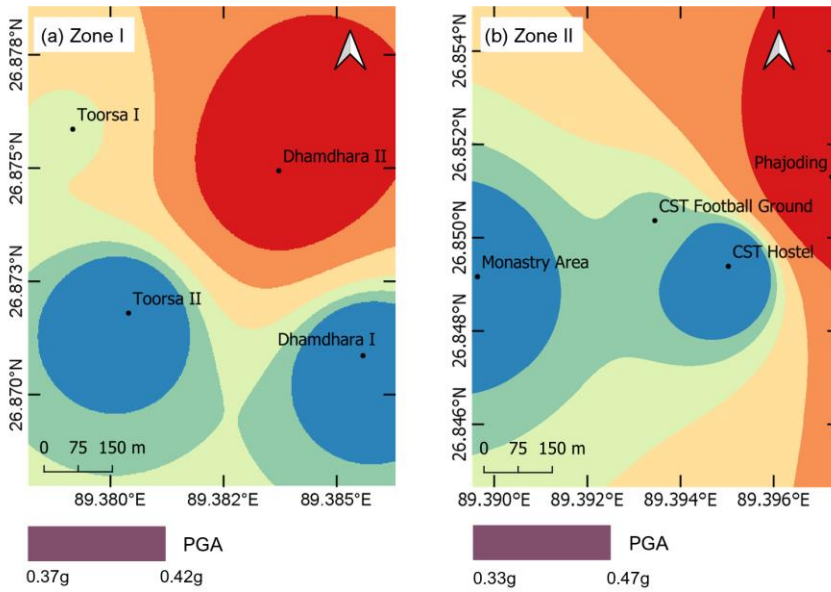


Figure 18: PGA distribution map of input motion M4 Northridge earthquake, (a) Toorsa and Dhamdhara in Zone I, (b) Rinchenjing in Zone II.

2.5. Conclusions

Using 1D site response analysis, we perform sensitivity of various input motions. The study concludes the following: This study shows the sensitivity of the various input motions using a 1D seismic response analysis. The overall significance of this study can be concluded as follows:

- The trend in the variation of ground motion parameters such as PGA, PGD, PGV_r and SA_r as expected, projects an increasing order in terms of the with ground motion intensity as expected. The correlation analysis and linear regression models provided the enhanced characteristics of input motion propagation, indicating possible use of earthquake PGA between 0.11 g and 0.33 g from 1 to 10 Hz frequency content. Further, the sensitivity analysis of the ground vibration. However, the uncertainty for each parameter is widely scattered, indicating the importance of the variability due to local soil conditions show potential interaction of the Northridge earthquake to local soils in Phuentsholing.
- The surface PGA in the investigation area of site classification type B shows about 0.1 g to 0.15 g for the earthquake of low intensity, 0.23 g to ~ 0.38 g for the earthquake of medium intensity, and more than 0.43 g for an earthquake of higher intensity earthquakes such as the 1992 Petrolia earthquake high PGA earthquakes.

Formatted: Space Before: 12 pt, After: 0 pt

Commented [rev22]: Again I'm not able to locate this maps ...

Commented [KT23R22]: These is the investigated area Zone I&II which is shown in box in Fig 2.

455 The result shows a higher spectral acceleration ~~of the soil profile~~ in a period range from 0.3 s to 3.0 sec with
 456 approximately 0.14 g to 1.62 g peak spectral acceleration.

- 457 • The critical range of the fundamental natural period is roughly between 0.9 sec to ~ 5.0 sec with the highest
 458 range of seismic wave amplification being between ~ 2.8 to 6.2. In Phajoding, the significance of
 459 amplification is comparatively less at ~ 1.7 between 0.4 s and 1.0 s due to a much stiffer soil deposit ($V_{s,30}$ =
 460 584.76 m/s) and a shallow engineering bedrock at 150 m. ~~This suggests that the low-rise buildings are more
 461 vulnerable and can see stronger vibrations than the high-rise buildings in Phajoding, however, overall effects
 462 on tall buildings cannot be neglected.~~
- 463 • ~~In the present seismic response analysis, the ground response of various strong ground motions with varying
 464 ground shaking intensity as an input motion. This study indicated show some anomalies to local soils and in
 465 seismic site effects due to input motion. Therefore, an appropriate appropriate proper ground motion
 466 characterization is recommended when the input motions are selected, especially while performing a for site-
 467 specific seismic analysis. The high Fourier amplitude characteristics at low frequency have a larger greater
 468 tendency to anomalies reflect anomalies in response parameters, e.g., input motion M1, M5 and M6, on
 469 bedrock response spectra have larger impacts in low periods and the response from M6 is evident from the
 470 current study. In other words, matching the frequency content and earthquake PGA gives a reliable estimate
 471 of seismic site effects. In other words, the frequency content of the ground motion and the variability of
 472 amplification would undermine the proper estimation of seismic site effects.~~

473 **3. Appendix A: Surface motion parameters**

474 **4. Annotations**

- 475 P = Profile number
 476 M = Motion number
 477 G_{rms} = Root mean square acceleration
 478 t_a = Bracketed duration
 479 D = Significant duration
 480 CAV = ~~Cumulative~~Cumulative absolute velocity
 481 SA = Spectral acceleration
 482 StDev = Standard deviation

483 **Table A1.** Additional surface motion parameters in Zone I.

P	M	PV (m/s)	PD (m)	G_{rms} (g)	t_a (s)	D5-95 (s)	D5-75 (sec)	CAV (g-s)	SA @ 1.0 s (g)
1	1	0.173	0.040	0.022	1.360	7.980	2.660	0.209	0.096
1	2	0.170	0.048	0.033	6.000	9.080	4.100	0.318	0.181
1	3	0.201	0.064	0.043	15.580	28.740	10.200	1.116	0.214
1	4	0.200	0.046	0.100	14.160	8.530	4.450	0.934	0.166
1	5	0.397	0.120	0.071	29.340	24.580	10.420	1.580	0.649

Formatted: No bullets or numbering

Formatted: Indent: Left: 0.25", No bullets or numbering

1	6	0.876	0.230	0.090	16.460	12.100	5.890	1.055	0.763
2	1	0.175	0.040	0.024	1.380	7.760	2.620	0.216	0.099
2	2	0.169	0.047	0.035	6.000	9.060	4.020	0.328	0.192
2	3	0.213	0.064	0.043	29.280	28.760	10.520	1.134	0.231
2	4	0.210	0.046	0.099	14.150	8.520	4.440	0.914	0.182
2	5	0.419	0.119	0.074	29.340	24.580	10.360	1.625	0.727
2	6	0.877	0.228	0.097	16.440	11.920	5.910	1.136	0.908
3	1	0.170	0.039	0.023	1.380	7.980	2.720	0.210	0.093
3	2	0.164	0.047	0.034	6.000	9.080	4.100	0.323	0.176
3	3	0.197	0.064	0.044	29.280	28.040	9.820	1.139	0.210
3	4	0.204	0.046	0.106	14.160	8.490	4.430	0.977	0.162
3	5	0.414	0.118	0.073	29.340	24.580	10.440	1.626	0.645
3	6	0.855	0.223	0.090	16.460	12.060	5.850	1.058	0.767
4	1	0.203	0.095	0.024	0.980	7.820	2.580	0.219	0.108
4	2	0.201	0.065	0.034	6.000	9.380	3.880	0.326	0.204
4	3	0.238	0.072	0.042	29.340	29.300	10.540	1.125	0.243
4	4	0.219	0.051	0.097	12.200	8.170	4.080	0.870	0.180
4	5	0.417	0.135	0.065	25.900	24.580	10.180	1.455	0.685
4	6	0.941	0.282	0.087	14.800	12.150	6.000	1.028	0.712
	Mean	0.346	0.097	0.060	15.222	15.135	6.259	0.872	0.358
	Median	0.283	0.078	0.053	10.276	13.150	5.545	0.703	0.269
	StDev	0.256	0.071	0.029	10.088	8.330	3.021	0.472	0.271
	84 th Percentile	0.509	0.146	0.090	30.026	22.042	9.121	1.450	0.570
	16 th Percentile	0.157	0.042	0.031	3.517	7.845	3.371	0.341	0.127

484

485 **Table A2.** Additional surface motion parameters in Zone II.

P	M	PV (m/s)	PD (m)	G_{rms} (g)	t_a (s)	D5-95 (s)	D5-75 (s)	CAV (g-s)	SA @ 1.0 sec (g)
1	1	0.181	0.043	0.024	1.380	7.840	2.600	0.215	0.104
1	2	0.182	0.048	0.035	6.000	8.960	4.000	0.325	0.197
1	3	0.215	0.066	0.043	29.320	28.800	10.480	1.135	0.231
1	4	0.214	0.047	0.097	12.200	8.270	4.170	0.879	0.179
1	5	0.404	0.124	0.072	29.360	24.600	10.380	1.598	0.677
1	6	0.936	0.244	0.095	16.470	12.060	5.770	1.106	0.816
2	1	0.186	0.041	0.024	1.380	7.760	2.540	0.212	0.103
2	2	0.186	0.046	0.035	5.980	8.940	3.900	0.322	0.199
2	3	0.217	0.067	0.042	19.000	28.900	10.520	1.101	0.232
2	4	0.211	0.047	0.090	12.190	8.300	4.190	0.815	0.177

2	5	0.393	0.126	0.070	29.340	24.580	10.340	1.557	0.686
2	6	0.943	0.250	0.096	16.450	11.920	5.800	1.101	0.839
3	1	0.158	0.037	0.021	1.360	8.060	3.020	0.202	0.078
3	2	0.149	0.045	0.031	6.000	9.360	4.520	0.317	0.152
3	3	0.178	0.062	0.044	17.040	27.420	9.720	1.116	0.175
3	4	0.182	0.043	0.111	16.880	8.640	4.610	1.056	0.135
3	5	0.406	0.112	0.076	29.340	24.400	10.720	1.690	0.551
3	6	0.830	0.218	0.092	18.050	11.900	5.390	1.103	0.704
4	1	0.184	0.041	0.023	0.960	7.800	2.580	0.209	0.101
4	2	0.183	0.048	0.034	6.000	8.940	3.960	0.319	0.195
4	3	0.212	0.066	0.041	18.960	28.840	10.520	1.084	0.227
4	4	0.209	0.047	0.091	12.200	8.300	4.190	0.832	0.175
4	5	0.391	0.125	0.069	29.340	24.580	10.340	1.530	0.672
4	6	0.905	0.243	0.091	16.440	11.990	5.870	1.056	0.793
	Mean	0.344	0.093	0.060	14.652	15.048	6.255	0.870	0.350
	Median	0.278	0.074	0.053	10.022	13.070	5.537	0.698	0.261
	StDev	0.263	0.071	0.029	9.536	8.295	3.052	0.480	0.268
	84 th Percentile	0.506	0.140	0.090	28.804	21.920	9.109	1.451	0.559
	16 th Percentile	0.153	0.039	0.031	3.487	7.793	3.365	0.335	0.122

486

487 **Data availability**

488 All the data used in this study are presented in the paper.

489 **Author contribution**

490 Conceptualization (KT), Data curation (KT), Formal analysis (KT), Funding acquisition (KRA),
491 Methodology (KT, DG and GF), Resources (KT, DG and KRA), Software and visualization (KT), Writing –
492 original draft preparation (KT), Writing – review & editing (DG, NC, GF and KRA).

493 **Competing interests**

494 The authors declare that they have no competing interests.

495 **5. Acknowledgements**

496 The authors are thankful to Phuentsholing Thromde (Municipal office) for providing additional geotechnical data.

497 **6. References**

498 [Anbazhagan, P., and Sitharam, T. G.: Seismic microzonation of Bangalore, India, Journal of Earth System](#)
499 [Science, 117, 833–852, https://doi.org/10.1007/s12040-008-0071-5, 2008.](#)

Formatted: Indent: Left: 0", Hanging: 0.25", No bullets or numbering

Formatted: Indent: Left: 0", Hanging: 0.25", No bullets or numbering

500 Ansal A., and Tönük G.: Source and Site Factors in Microzonation. In: Pitilakis K.D. (eds) Earthquake
501 Geotechnical Engineering, Geotechnical, Geological and Earthquake Engineering, vol 6. Springer, Dordrecht,
502 https://doi.org/10.1007/978-1-4020-5893-6_4, 2007.

503 Bajaj, K., and Anbazhagan, P.: Site Amplification Factors and Acceleration Response Spectra for Shallow
504 Bedrock Sites Application to Southern India, Journal of Earthquake Engineering, 26(1), 1–21,
505 <https://doi.org/10.1080/13632469.2020.1754308>, 2020.

506 Bala, A., Balan, S. F., Ritter, J. R. R., Hannich, D., Huber, G., and Rohn, J.: Seismic site effects based on in situ
507 borehole measurements in Bucharest, Romania, Proceedings of the International Symposium on Strong Vrancea
508 Earthquake and Risk Mitigation, 1, 15, 2007.

509 Berthet, T., Hetényi, G., Cattin, R., Sapkota, S. N., Champollion, C., Kandel, T., Doerflinger, E., Drukpa, D.,
510 Lechmann, S., and Bonnín, M.: Lateral uniformity of India Plate strength over central and eastern Nepal,
511 Geophysical Journal International, 195(3), 1481–1493, <https://doi.org/10.1093/gji/ggt357>, 2013.

512 Bhutani, M., and Naval, S.: Preliminary amplification studies of some sites using different earthquake motions,
513 Civil Engineering Journal (Iran), 6(10), 1906–1921, <https://doi.org/10.28991/cej-2020-03091591>, 2020.

514 Bommer, J. J., and Martinez-Pereira, A.: Strong-motion parameters: definition, usefulness and predictability, 12th
515 World Conference on Earthquake Engineering, 1–8, <http://www.iitk.ac.in/nicee/wcee/article/0206.pdf>, 2000.

516 Bradley, B. A.: Empirical correlation of PGA, spectral acceleration and spectrum intensities from active shallow
517 crustal earthquakes, Earthquake Engineering and Structural Dynamics, 40(15), 1–15. <https://doi.org/10.1002/eqe>,
518 2011.

519 Chamlagain D., and Gautam D.: Seismic Hazard in the Himalayan Intermontane Basins: An Example from
520 Kathmandu Valley, Nepal, In: Nibanupudi H., Shaw R. (eds) Mountain Hazards and Disaster Risk Reduction,
521 Disaster Risk Reduction (Methods, Approaches and Practices), Springer, Tokyo, [https://doi.org/10.1007/978-4-](https://doi.org/10.1007/978-4-431-55242-0_5)
522 431-55242-0_5, 2015.

523 Chavez-Garcia, F. J., Pedotti, G., Hatzfeld, D., and Bard, P. Y.: An experimental study of site effects near
524 Thessaloniki (northern Greece), Bulletin - Seismological Society of America, 80(4), 784–806, 1990.

525 Chettri, N., Gautam, D., and Rupakhety, R.: From Tship Chim to Pa Chim: Seismic vulnerability and
526 strengthening of Bhutanese vernacular buildings, In R. Rupakhety and D. Gautam (Ed.), Masonry Construction in
527 Active Seismic Regions (1st ed. Ca, Issue May, pp. 253–288), Elsevier, [https://doi.org/10.1016/c2019-0-02453-](https://doi.org/10.1016/c2019-0-02453-3)
528 3, 2021. a

529 Chettri, N., Gautam, D., and Rupakhety, R.: Seismic vulnerability of vernacular residential buildings in Bhutan,
530 Journal of Earthquake Engineering, 26(1), 1–16. <https://doi.org/10.1080/13632469.2020.1868362>, 2021. b

531 Darendeli, M. B.: Development of a New Family of Normalized Modulus Reduction and Material Damping
532 Curves, Dept. of Civil Eng., Univ. of Texas, Austin, 2001

533 Dobry, R., and Vucetic, M.: Dynamic properties and seismic response of soft clay deposits, International
534 Symposium on Geotech., Eng. of Soft Soils, Mexico, 2(January 1987), 51–87, 1982.

535 Douglas, J.: Selection of strong-motion records for use as input to the structural models of VEDA, BRGM, 2006.

536 Drukpa, D., Velasco, A. A., and Doser, D. I.: Seismicity in the Kingdom of Bhutan (1937-2003): Evidence for
537 crustal transcurrent deformation, *Journal of Geophysical Research: Solid Earth*, 111(6), 1–14,
538 <https://doi.org/10.1029/2004JB003087>, 2006.

539 EduPro Civil Systems Inc.: ProShake: Ground Response Analysis Program 2.0, User's Manual. 2017.

540 Gautam, D.: Mapping surface motion parameters and liquefaction susceptibility in Tribhuvan International
541 Airport, Nepal, *Geomatics, Natural Hazards and Risk*, 8(2), 1173–1184,
542 <https://doi.org/10.1080/19475705.2017.1305993>, 2017.

543 Gautam, D., and Chamlagain, D.: Preliminary assessment of seismic site effects in the fluvio-lacustrine sediments
544 of Kathmandu valley, Nepal, *Natural Hazards*, 81(3), 1745–1769, <https://doi.org/10.1007/s11069-016-2154-y>,
545 2016.

546 Gautam, D., Forte, G., and Rodrigues, H.: Site effects and associated structural damage analysis in Kathmandu
547 Valley, Nepal. *Earthquake and Structures*, 10(5), 1013–1032, <https://doi.org/10.12989/eas.2016.10.5.1013>, 2016.

548 Housner, G.W.: Behavior of structures during earthquakes, *Journal of the Engineering Mechanics Division*,
549 *ASCE*, 85(14), 109-129, 1959.

550 ISSMGE.: Manual for zonation on seismic geotechnical hazards. In: Technical committee for earthquake
551 geotechnical engineering, TC4, international society for soil mechanics and geotechnical engineering, The
552 Japanese Geotechnical Society, Tokyo, 1999.

553 IS:1893.: Criteria for Earthquake Resistant Design of Structures - General Provisions and Buildings Part-1, Bureau
554 of Indian Standards, New Delhi, Part 1, 1–39, 2002.

555 Jishnu, R. B., Naik, S. P., Patra, N. R., and Malik, J. N.: Ground response analysis of Kanpur soil along Indo-
556 Gangetic Plains, *Soil Dynamics and Earthquake Engineering*, 51(2013), 47–57,
557 <https://doi.org/10.1016/j.soildyn.2013.04.001>, 2013.

558 Kirtas, E., Koliopoulos, P., Kappos, A., Theodoulidis, N., Savvaidis, A., Margaris, B., and Rovithis, E.:
559 Identification of earthquake ground motion using site effects analysis in the case of Serres city, Greece,
560 *International Journal of Civil Engineering and Architecture*, 2(1), 20–27, 2015.

561 Kramer, S. L.: *Geotechnical Earthquake Engineering*, Prentice Hall, 1996.

562 Kramer, S. L., Arduino, P., and Sideras, S. S.: *Earthquake ground motion selection*, The State of Washington
563 Department of Transportation, 2012.

564 Long, S., and McQuarrie, N.: Placing limits on channel flow: Insights from the Bhutan Himalaya, *Earth and*
565 *Planetary Science Letters*, 290(3–4), 375–390, <https://doi.org/10.1016/j.epsl.2009.12.033>; 2010.

566 Lopez-Caballero, F., Gelis, C., Regnier, J., and Bonilla, L. F.: Site response analysis including earthquake input
567 ground motion and soil dynamic properties variability, 15th World Conference on Earthquake Engineering, 2012.

568 Licata, V., Forte, G., d'Onofrio, A., Santo, A., Silvestri, F.: A multi-level study for the seismic microzonation of
569 the Western area of Naples (Italy), *Bulletin of Earthquake Engineering*, 17(9), 4711–4741, 2019.

570 McQuarrie, N., Long, S. P., Tobgay, T., Nesbit, J. N., Gehrels, G., and Ducea, M. N.: Documenting basin scale,
571 geometry and provenance through detrital geochemical data: Lessons from the Neoproterozoic to Ordovician
572 Lesser, Greater, and Tethyan Himalayan strata of Bhutan, *Gondwana Research*, 23(4), 1491–1510,
573 <https://doi.org/10.1016/j.gr.2012.09.002>, 2013.

574 Naik, S. P., and Patra, N. R.: Generation of Liquefaction Potential Map for Kanpur City and Allahabad City of
575 Northern India: An Attempt for Liquefaction Hazard Assessment, *Geotechnical and Geological Engineering*,
576 36(1), 293–305, <https://doi.org/10.1007/s10706-017-0327-4>, 2018.

577 Nath, S. K., and Thingbaijam, K. K. S.: Seismic hazard assessment - A holistic microzonation approach, *Natural
578 Hazards and Earth System Science*, 9(4), 1445–1459, <https://doi.org/10.5194/nhess-9-1445-2009>, 2009.

579 Panjamani, A., Katukuri, A. K., Reddy, G. R., Moustafa, S. S. R., and Al-Arifi, N. S. N.: Seismic site classification
580 and amplification of shallow bedrock sites, *PLoS ONE*, 13(12), 1–22,
581 <https://doi.org/10.1371/journal.pone.0208226>, 2018.

582 Puri, N., Jain, A., Mohanty, P., and Bhattacharya, S.: Earthquake Response Analysis of Sites in State of Haryana
583 using DEEPSOIL Software, *Procedia Computer Science*, 125(January), 357–366,
584 <https://doi.org/10.1016/j.procs.2017.12.047>, 2018.

585 Seed, H. B., and Idriss, I. M.: Soil Moduli and Damping Factors for Dynamic Response Analyses [Report No.
586 EERC 70-10], Earthquake Engineering Research Centre, University of California, Berkeley,
587 <https://ntrl.ntis.gov/NTRL/dashboard/searchResults/titleDetail/PB197869.xhtml>, 1970.

588 Seed, H. B., Wong, R. T., Idriss, I. M., and Tokimatsu, K.: Moduli and Damping Factors for Dynamic Analyses
589 of Cohesionless Soils, *Journal of Geotechnical Engineering*, 112(11), 1016–1032, 1986.

590 Shafiee, A., Kamalian, M., Jafari, M. K., and Hamzehloo, H.: Ground motion studies for microzonation in Iran,
591 *Natural Hazards*, 59(1), 481–505, <https://doi.org/10.1007/s11069-011-9772-1>, 2011.

592 Shiuly, A., and Narayan, J. P.: Deterministic seismic microzonation of Kolkata city. *Natural Hazards*, 60(2), 223–
593 240, <https://doi.org/10.1007/s11069-011-0004-5>, 2012.

594 Sil, A., and Haloi, J.: Site-specific ground response analysis of a proposed bridge site over Barak River along
595 Silchar Bypass Road, India, *Innovative Infrastructure Solutions*, 3(1), <https://doi.org/10.1007/s41062-018-0167->
596 y, 2018.

597 Sitharam, T. G.: Seismic Microzonation: Principles, Practices and Experiments, *Electronic Journal of
598 Geotechnical Engineering*, 1–58, 2008.

599 Sitharam, T. G., Anbazhagan, P., Mahesh, G. U., Bharathi, K., and Reddy, P. N.: Seismic Hazard Studies Using
600 Geotechnical Borehole Data and GIS, *Symposium on Seismic Hazard Analysis and Microzonation*, 341–358,
601 2005.

602 Stevens, V. L., De Risi, R., Le Roux-Mallouf, R., Drukpa, D., and Hetényi, G.: Seismic hazard and risk in Bhutan,
603 *Natural Hazards*, 104(3), 2339–2367, <https://doi.org/10.1007/s11069-020-04275-3>, 2020.

604 Tempa, K., and Chettri, N.: Comprehension of Conventional Methods for Ultimate Bearing Capacity of Shallow
605 Foundation by PLT and SPT in Southern Bhutan, *Civil Engineering and Architecture*, 9, 375–385,
606 <https://doi.org/10.13189/cea.2021.090210>, 2021.

607 Tempa, K., Chettri, N., Gurung, L., and Gautam, D.: Shear wave velocity profiling and ground response analysis
608 in Phuentsholing, Bhutan, *Innovative Infrastructure Solutions*, 6(2), 1–16, <https://doi.org/10.1007/s41062-020-020-00420-w>, 2021.

610 Tempa, K., Chettri, N., Sarkar, R., Saha, S., Gurung, L., Dendup, T., and Nirola, B. S.: Geotechnical parameter
611 assessment of sediment deposit: A case study in Pasakha, Bhutan, *Cogent Engineering*, 8(1), 1–21,
612 <https://doi.org/10.1080/23311916.2020.1869366>, 2021.

613 Tempa, K., Sarkar, R., Dikshit, A., Pradhan, B., Simonelli, A. L., Acharya, S., and Alamri, A. M.: Parametric
614 study of local site response for bedrock ground motion to earthquake in Phuentsholing, Bhutan, *Sustainability*
615 (Switzerland), 12(13), 1–20, <https://doi.org/10.3390/su12135273>, 2020.

616 Vucetic, M., and Dobry, R.: Effect of Soil Plasticity on Cyclic Response. *Journal of Geotechnical Engineering*,
617 117(1), 89–107, <http://sokocalo.engr.ucdavis.edu/~jeremic/PAPERSlocalREPO/CM1769.pdf>, 1991.

618 Wyss, M., and Rosset, P.: Mapping seismic risk: The current crisis. *Natural Hazards*, 68(1), 49–52,
619 <https://doi.org/10.1007/s11069-012-0256-8>, 2013.

620 Zafarani, H., Ghafoori, S. M. M., Soghrat, M. R., and Shafiee, M.: Spatial correlation of peak ground motions and
621 pseudo-spectral acceleration based on the sarpol-e-zahab mw 7.3, 2017 earthquake data, *Annals of Geophysics*,
622 63(4), 1–15, <https://doi.org/10.4401/ag-8349>, 2020.